

1.1 Crystals, Lattices, and Cells

A crystal is composed of a periodic repetition of identical groups of atoms: A group is called *basis*. The corresponding crystal lattice is obtained by replacing each group of atoms by a representative point, as shown in Fig. 1.1. A crystal can also be called *lattice with a basis*. When the basis is composed of a single atom, the corresponding lattice is called *monoatomic*. In a *Bravais lattice*, the position \mathbf{R} of all points in the lattice can be written as :

$$\mathbf{R} = n_1\mathbf{a}_1 + n_2\mathbf{a}_2 + n_3\mathbf{a}_3, \quad (1.1)$$

where \mathbf{a}_1 , \mathbf{a}_2 , and \mathbf{a}_3 are three noncoplanar translation vectors called the *primitive vectors*, and n_1 , n_2 , and n_3 are arbitrary (positive or negative) integers. We note that for a given Bravais lattice, the choice of the primitive vectors is not unique. The Bravais lattice looks exactly the same when viewed from any lattice point. Not only the arrangement of points but also the orientation must be exactly the same from every point in a Bravais lattice. No rotations are needed to reach each lattice point. Therefore, two points in the lattice, whose position vectors are given by \mathbf{r} and $\mathbf{r}' = \mathbf{r} + \mathbf{R}$, are completely equivalent environmentally. For example, the two-dimensional honeycomb lattice as shown in Fig. 1.2 is not a Bravais lattice. Indeed, the lattice looks the same when it is viewed from points A and C, but not when it is viewed from point B: In this case, the lattice appears rotated by 180° . We note that, for example, graphene consists of a single layer of carbon atoms arranged in a two-dimensional honeycomb structure.

A lattice can be constructed by infinite repetitions, by translations, of a single cell without any overlapping. This cell can be primitive or nonprimitive (or conventional). Primitive and conventional cells are not uniquely determined, as clearly illustrated in Fig. 1.3. The primitive cell has the minimum possible volume, given by

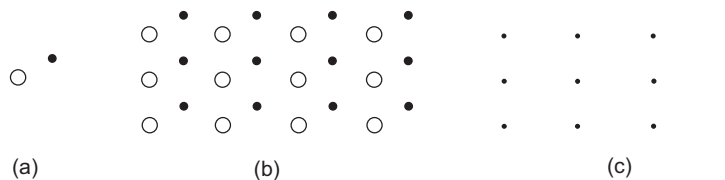


Figure 1.1

(a) Basis composed of two different atoms, (b) bidimensional crystal, and (c) corresponding lattice.

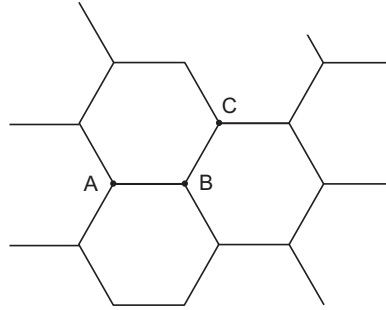


Figure 1.2 A two-dimensional honeycomb lattice is not a Bravais lattice.

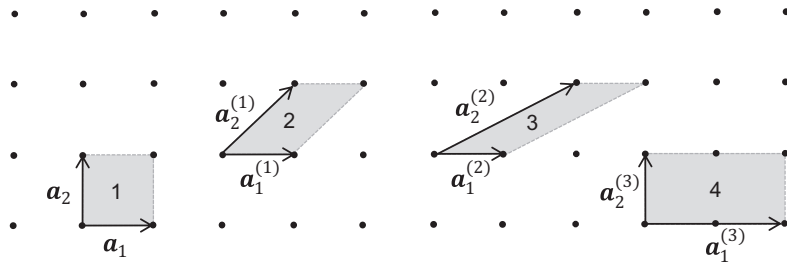


Figure 1.3 Two-dimensional lattice: cells 1, 2, and 3 are primitive cells. Cell 4 is not primitive.

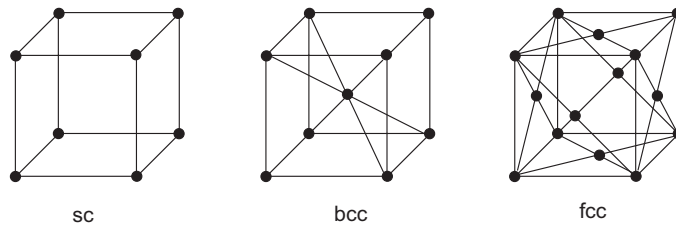
$$V_u = \mathbf{a}_1 \cdot (\mathbf{a}_2 \times \mathbf{a}_3), \quad (1.2)$$

and contains exactly one lattice point. Therefore, in Fig. 1.3, which refers to a two-dimensional case, the cells 1–3 are all primitive cells: They have the same area and contain $4 \cdot \frac{1}{4} = 1$ lattice point. The primitive cell contains the minimum possible number of atoms, and there is always a lattice point per primitive cell. Cell 4 is not primitive: Its area is twice the area of the primitive cell and contains $4 \cdot \frac{1}{4} + 2 \cdot \frac{1}{2} = 2$ lattice points. Not all points in the lattice are linear combinations of $\mathbf{a}_1^{(3)}$ and $\mathbf{a}_2^{(3)}$ with integral coefficients ($\mathbf{a}_1^{(3)}$ and $\mathbf{a}_2^{(3)}$ are not the primitive vectors). In some cases, it is more convenient to consider conventional unit cells, with larger volumes (integer multiple of that of the primitive cell) but characterized by the same symmetry of the lattice.

Without entering into any detail about group theory, we can say that all the possible lattice structures are determined by the symmetry group that describes their properties. A lattice structure can be transformed into itself not only by the translations described by Eq. 1.1, which define the translational group, but also by many other symmetry operations. The symmetry operations transforming a lattice into itself keeping at least one point fixed form a group called the *point group*. In the case of three-dimensional structures, the point symmetry gives rise to 14 types of lattices, which can be classified depending on the relationships between the amplitudes of the vectors \mathbf{a}_i and the angles α , β , and γ between them.

Table 1.1 The 14 lattice systems in three dimensions (the last column shows the amplitudes a_i and the angles between vectors \mathbf{a}_i of the unit cell).

System	Number of lattices	Amplitudes a_i and angles
Triclinic	1	$a_1 \neq a_2 \neq a_3$ $\alpha \neq \beta \neq \gamma$
Monoclinic	2	$a_1 \neq a_2 \neq a_3$ $\alpha = \gamma = 90^\circ, \beta \neq 90^\circ$
Orthorhombic	4	$a_1 \neq a_2 \neq a_3$ $\alpha = \beta = \gamma = 90^\circ$
Tetragonal	2	$a_1 = a_2 \neq a_3$ $\alpha = \beta = \gamma = 90^\circ$
Cubic	3	$a_1 = a_2 = a_3$ $\alpha = \beta = \gamma = 90^\circ$
Trigonal	1	$a_1 = a_2 = a_3$ $\alpha = \beta = \gamma < 120^\circ, \neq 90^\circ$
Hexagonal	1	$a_1 = a_2 \neq a_3$ $\alpha = \beta = 90^\circ, \gamma = 120^\circ$

**Figure 1.4** Cubic lattices: (sc) simple cubic, (bcc) body-centered cubic, and (fcc) face-centered cubic.

As reported in Table 1.1, the 14 types of lattices can be grouped in one triclinic, two monoclinic, four orthorhombic, two tetragonal, three cubic, one trigonal, and one hexagonal lattices.

Many semiconductors are characterized by a cubic lattice or by an hexagonal lattice. There are three types of cubic lattices: simple cubic (sc), body-centered cubic (bcc), and face-centered cubic (fcc), whose unit cells are shown in Fig. 1.4. Note that only the sc is a primitive cell, with volume a^3 and one lattice point per cell ($8 \times \frac{1}{8}$). The bcc lattice can be obtained from the sc by placing a lattice point at the center of the cube. The conventional cell is the cube with edge a . It has two lattice points per unit cell ($8 \times \frac{1}{8} + 1$). In terms of the cube edge a , a set of primitive vectors can be written as:

$$\begin{aligned}
 \mathbf{a}_1 &= \frac{a}{2}(\mathbf{u}_x + \mathbf{u}_y - \mathbf{u}_z) \\
 \mathbf{a}_2 &= \frac{a}{2}(-\mathbf{u}_x + \mathbf{u}_y + \mathbf{u}_z) \\
 \mathbf{a}_3 &= \frac{a}{2}(\mathbf{u}_x - \mathbf{u}_y + \mathbf{u}_z),
 \end{aligned} \tag{1.3}$$

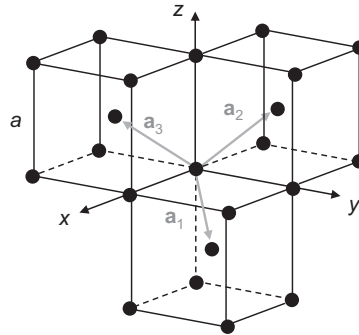


Figure 1.5 Set of primitive vectors for a body-centered cubic lattice.

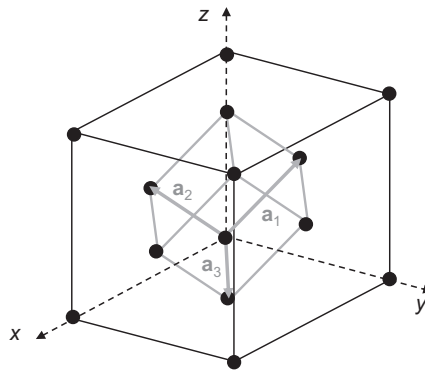


Figure 1.6 Primitive vectors and primitive cell of the face-centered cubic lattice.

where \mathbf{u}_x , \mathbf{u}_y , and \mathbf{u}_z are the unit vectors of the x , y , and z axes, as shown in Fig. 1.5. The corresponding primitive cell, with volume $a^3/2$, contains by definition only one lattice point. This primitive cell does not have an obvious relation with the point symmetry (cubic) of the lattice. For this reason, it is useful to consider a unit cell larger than the primitive cell and with the same symmetry of the crystal. For a bcc lattice, the unit cell is a cube with edge a , with a volume which is twice the volume of the primitive cell. The bcc lattice can also be considered as an sc lattice with a two-point basis $0, (a/2)(\mathbf{u}_x + \mathbf{u}_y + \mathbf{u}_z)$.

The fcc Bravais lattice can be obtained from the sc lattice by adding a point in the center of each face. The fcc structure has lattice points on the faces of the cube, so that they are shared between two cells: The total number of lattice points in the cell is $4 (8 \times \frac{1}{8} + 6 \times \frac{1}{2})$. A particular set of primitive vectors is (see Fig. 1.6):

$$\begin{aligned} \mathbf{a}_1 &= \frac{a}{2}(\mathbf{u}_y + \mathbf{u}_z) \\ \mathbf{a}_2 &= \frac{a}{2}(\mathbf{u}_z + \mathbf{u}_x) \\ \mathbf{a}_3 &= \frac{a}{2}(\mathbf{u}_x + \mathbf{u}_y). \end{aligned} \quad (1.4)$$

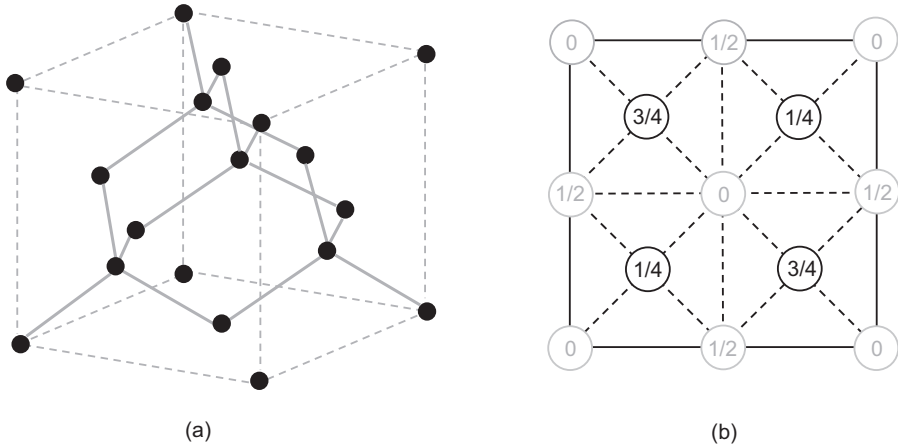


Figure 1.7

(a) Crystal structure of diamond; the solid lines show the tetrahedral bond geometry; (b) atomic position in the cubic cell projected on a cube face. The fractions correspond to the height above the cube face in the unit of the cube edge a ; the black and gray circles correspond to the two interpenetrating fcc lattices, which generate the diamond structure.

The primitive cell has a volume of $a^3/4$ and contains one lattice point. Also in this case, the unit cell is generally assumed as a cube of edge a , with a volume which is four times the volume of a primitive cell. The fcc can be described as an sc lattice with a four-point basis $0, (a/2)(\mathbf{u}_x + \mathbf{u}_y), (a/2)(\mathbf{u}_y + \mathbf{u}_z), (a/2)(\mathbf{u}_z + \mathbf{u}_x)$. We recall that the numbers giving the size of the unit cell (e.g., the number a in the case of a cubic crystal) are called the lattice constants.

Many important semiconductors, for example, silicon and germanium, have a *diamond structure*, which is the lattice formed by the carbon atoms in a diamond crystal. This structure consists of identical atoms that occupy the lattice points of two interpenetrating fcc lattices, which are displaced from each other along the body diagonal of the cubic cell by one quarter the length of the diagonal, as shown in Fig. 1.7. It can be seen as an fcc lattice with a two-point basis $0, (a/4)(\mathbf{u}_x + \mathbf{u}_y + \mathbf{u}_z)$. The four nearest neighbors of each point are on the vertices of a regular tetrahedron. Note that the diamond lattice is not a Bravais lattice, since it does not look exactly the same when it is viewed from the two nearest-neighbor points. Since the unit cell of an fcc structure contains four lattice points, the unit cell of the diamond structure contains eight lattice points. In this case, it is not possible to choose a primitive cell in such a way that the basis of diamond contains only one atom. When the atoms that occupy one of the two fcc structures are different from the atoms occupying the other, the structure is called the *zinc-blende* structure. Several semiconductors are characterized by this structure, such as GaAs, AlAs, and many others.

Largely used semiconductors, such as GaN, AlN, BN, and SiC, have a hexagonal close-packed (hcp) structure (wurtzite structure) as shown in Fig. 1.8. Also, the hcp lattice is not a Bravais lattice. This lattice can be seen as two interpenetrating simple hexagonal Bravais lattices, displaced vertically by $c/2$ in the direction of the common c -axis and displaced

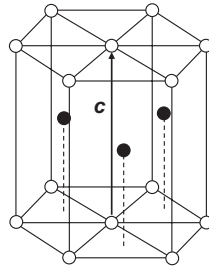


Figure 1.8 Atomic position in the hcp lattice.

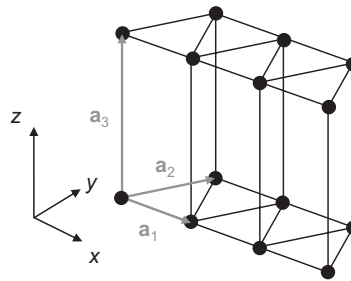


Figure 1.9 Simple hexagonal Bravais lattice.

in the horizontal plane in such a way that the points of one simple hexagonal lattice are placed above the centers of the triangles formed by the points of the other simple hexagonal lattice. Figure 1.9 shows a simple hexagonal Bravais lattice, which is obtained by stacking two-dimensional triangular Bravais lattices – one exactly above the other along a direction perpendicular to each two-dimensional lattice. This stacking direction is usually called the crystallographic c -axis. The primitive vectors can be written as:

$$\begin{aligned} \mathbf{a}_1 &= a\mathbf{u}_x \\ \mathbf{a}_2 &= \frac{a}{2}\mathbf{u}_x + \frac{\sqrt{3}}{2}a\mathbf{u}_y \\ \mathbf{a}_3 &= c\mathbf{u}_z. \end{aligned} \quad (1.5)$$

1.1.1 The Wigner–Seitz Cell

The primitive cell can also be chosen in such a way that it presents the full symmetry of the Bravais lattice. This can be achieved by considering the Wigner–Seitz cell. The mathematical definition is as follows: The Wigner–Seitz cell around a given lattice point is the spatial region that is closer to that particular lattice point than to any other lattice points. It can also be demonstrated that the Wigner–Seitz cell is a primitive cell. While for any given lattice there is an infinite number of possible primitive cells, there is only one Wigner–Seitz cell. The above definition does not refer to any particular choice of primitive

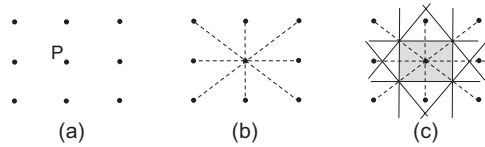


Figure 1.10 Construction of the Wigner–Seitz cell of a two-dimensional rectangular lattice.

vectors; for this reason, the Wigner–Seitz cell is as symmetrical as the Bravais lattice. The procedure for the construction of a Wigner–Seitz cell can be illustrated in the simple case of a two-dimensional rectangular lattice, as shown in Fig. 1.10(a). To determine the Wigner–Seitz cell about the lattice point P, we have first to draw the lines from P to all of its nearest neighbors (Fig. 1.10(b)) and then the bisectors to each of these lines (Fig. 1.10(c)). The Wigner–Seitz cell is the innermost region bounded by the perpendicular bisectors, as shown by the shaded region in Fig. 1.10(c). The same procedure can be applied in the case of a generic three-dimensional lattice.

1.2 The Reciprocal Lattice

In order to develop an analytic study of a crystalline solid, it is often useful to introduce the concept of a reciprocal lattice, which basically represents the Fourier transform of the Bravais lattice. The reciprocal lattice of the reciprocal lattice is the direct lattice. The reciprocal lattice provides a simple and useful basis for analyzing processes characterized by a “wave nature” in crystals, like the behavior of electrons and lattice vibrations, or the geometry of X-ray and electron diffraction patterns. Assuming a Bravais lattice defined by the primitive translation vectors ($\mathbf{a}_1, \mathbf{a}_2, \mathbf{a}_3$), the reciprocal lattice can be defined by introducing its primitive translation vectors ($\mathbf{b}_1, \mathbf{b}_2, \mathbf{b}_3$) in analogy with the lattice in a real space. The axis vectors of the reciprocal space can be written as:

$$\begin{aligned} \mathbf{b}_1 &= \frac{2\pi}{V_u} \mathbf{a}_2 \times \mathbf{a}_3 \\ \mathbf{b}_2 &= \frac{2\pi}{V_u} \mathbf{a}_3 \times \mathbf{a}_1 \\ \mathbf{b}_3 &= \frac{2\pi}{V_u} \mathbf{a}_1 \times \mathbf{a}_2, \end{aligned} \quad (1.6)$$

where V_u is the volume of the unit cell given by:

$$V_u = \mathbf{a}_1 \cdot (\mathbf{a}_2 \times \mathbf{a}_3). \quad (1.7)$$

The reciprocal lattice can be mapped by using the general translation vector \mathbf{G} given by:

$$\mathbf{G} = m_1 \mathbf{b}_1 + m_2 \mathbf{b}_2 + m_3 \mathbf{b}_3, \quad (1.8)$$

where $m_1, m_2,$ and m_3 are integers. Vector \mathbf{G} is called the reciprocal lattice vector. Note that each vector given by Eq. 1.6 is orthogonal to two-axis vectors of the crystal lattice, so that:

$$\mathbf{b}_i \cdot \mathbf{a}_j = 2\pi \delta_{ij}, \quad (1.9)$$

where δ_{ij} is the Kronecker delta symbol: $\delta_{ij} = 0$ for $i \neq j$ and $\delta_{ij} = 1$, for $i = j$. Moreover,

$$\mathbf{G} \cdot \mathbf{R} = 2\pi(n_1 m_1 + n_2 m_2 + n_3 m_3) = 2\pi \ell, \quad \ell = 0, \pm 1, \pm 2, \dots, \quad (1.10)$$

so that:

$$\exp(i \mathbf{G} \cdot \mathbf{R}) = 1. \quad (1.11)$$

Any function $f(\mathbf{r})$ with the periodicity of the crystal lattice, that is, $f(\mathbf{r} + \mathbf{R}) = f(\mathbf{r})$, can be expanded as:

$$f(\mathbf{r}) = \sum_{\mathbf{G}} f_{\mathbf{G}} e^{i\mathbf{G} \cdot \mathbf{r}}, \quad (1.12)$$

where:

$$f_{\mathbf{G}} = \frac{1}{V_u} \int_{cell} f(\mathbf{r}) e^{-i\mathbf{G} \cdot \mathbf{r}} d\mathbf{r}. \quad (1.13)$$

While vectors in the direct lattice have the dimension of length, the vectors in the reciprocal lattice have the dimension of $[\text{length}]^{-1}$. The reciprocal space is therefore the most convenient space for the wave vector \mathbf{k} . Since each point in the reciprocal space can be reached by the translation vector \mathbf{G} , it is evident that we can restrict our analysis to a unit cell defined by the vector \mathbf{b}_i . The Wigner–Seitz cell of the reciprocal lattice is called the *first Brillouin zone*. There are also the second, third, etc. Brillouin zones, at an increasing distance from the origin, all with the same volume. These higher order Brillouin zones can be translated into the first zone by adding suitable translation vector \mathbf{G} . A Wigner–Seitz cell in the reciprocal space can be constructed following the same procedure used in the real space. For example, in the simple case of a linear lattice, we have a single primitive vector in the direct space: $\mathbf{a}_1 = a\mathbf{u}_x$. From Eq. 1.9, it is obvious that the primitive vector in the reciprocal space is:

$$\mathbf{b}_1 = \frac{2\pi}{a} \mathbf{u}_x. \quad (1.14)$$

The corresponding translation vector is given by:

$$\mathbf{G} = m \frac{2\pi}{a} \mathbf{u}_x, \quad m = \pm 1, \pm 2, \dots \quad (1.15)$$

Following the rules for the construction of the first Brillouin zone, we have that this region extends from $k = -\pi/a$ to $k = \pi/a$.

Following the same procedure, it is possible to construct the first Brillouin zone for three-dimensional structures. For a sc lattice, where:

$$\mathbf{a}_1 = a\mathbf{u}_x, \quad \mathbf{a}_2 = a\mathbf{u}_y, \quad \mathbf{a}_3 = a\mathbf{u}_z, \quad (1.16)$$

by using Eq. 1.6, where $V_u = a^3$:

$$\mathbf{b}_1 = \frac{2\pi}{a} \mathbf{u}_x, \quad \mathbf{b}_2 = \frac{2\pi}{a} \mathbf{u}_y, \quad \mathbf{b}_3 = \frac{2\pi}{a} \mathbf{u}_z. \quad (1.17)$$

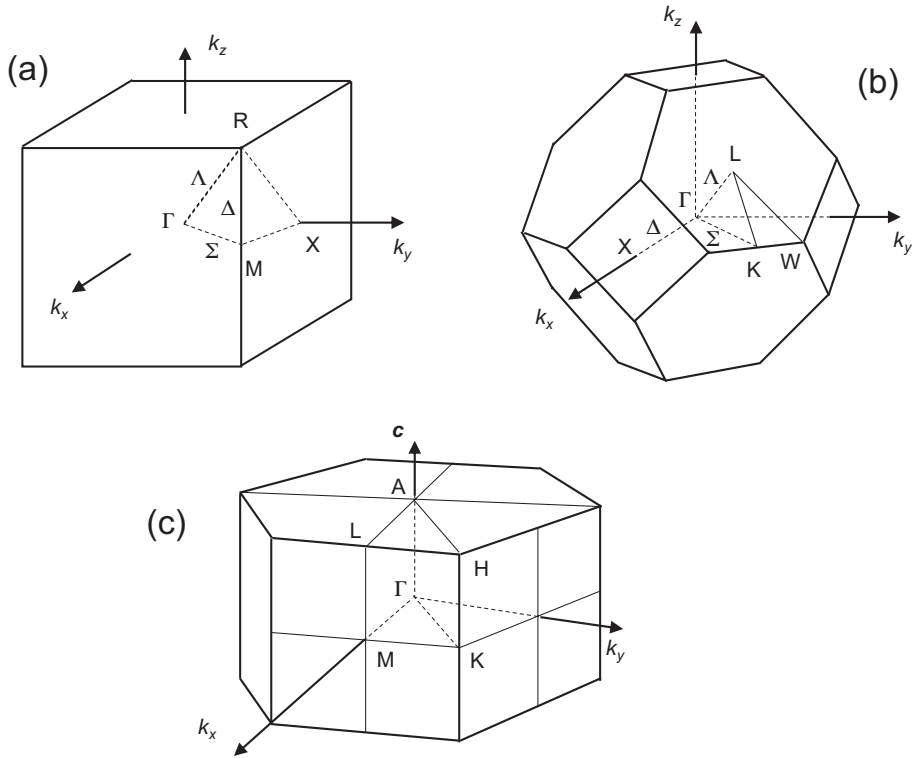


Figure 1.11 First Brillouin zone for (a) the sc lattice, (b) the fcc lattice, which forms the underlying Bravais lattice for the diamond and zinc-blende structures, and (c) the hexagonal wurtzite structure. Reported are the names of points and directions of high symmetry.

Therefore, the reciprocal lattice of an sc lattice with cubic primitive cell of edge a is an sc lattice with a cubic primitive cell of edge $2\pi/a$, and the first Brillouin zone is defined as follows:

$$-\frac{\pi}{a} \leq k_i \leq \frac{\pi}{a}, \quad i = x, y, z. \quad (1.18)$$

This is shown in Fig. 1.11(a). The center of the first Brillouin zone is always called the Γ -point. A typical convention is to call high-symmetry points and directions inside the Brillouin zone by Greek letters and high-symmetry points on the surfaces of the Brillouin zone by roman letters. For example, in the case of the fcc structure (see Fig. 1.11(b)), the three high-symmetry directions $[100]$, $[110]$, and $[111]$ are denoted by:

$$[100] \text{ direction: } \dot{\Gamma} \overline{\Delta} \dot{X}$$

$$[111] \text{ direction: } \dot{\Gamma} \overline{\Lambda} \dot{L}$$

$$[110] \text{ direction: } \dot{\Gamma} \overline{\Sigma} \dot{K}$$

The X -point at $(2\pi/a)(1,0,0)$ identifies the zone edge along the six equivalent $[100]$ directions. The L -point is at $(\pi/a)(1,1,1)$, and it is at the zone edge along the eight equivalent $[111]$ directions.

1.3 Electrons in a Periodic Crystal

After this brief overview of introductory concepts of solid-state physics, we will study the interactions of electrons with a periodic structure. We will consider bulk semiconductors, that is, semiconductors with spatial dimensions much larger than the de Broglie wavelength ($\lambda_B = h/p$, where p is the particle momentum) of the electrons involved in the interaction. In order to study the electronic and optical properties of the crystal, we have first to calculate the electronic wavefunctions and their energies inside the crystal. The system is described by the following Schrödinger equation:

$$\left[-\frac{\hbar^2}{2m_0} \nabla^2 + U(\mathbf{r}) \right] \psi(\mathbf{r}) = \mathcal{E} \psi(\mathbf{r}), \quad (1.19)$$

where $U(\mathbf{r})$ is a periodic potential due to the atoms periodically placed in the crystal lattice and to all interaction potentials between electrons. As a consequence of the crystal structure, $U(\mathbf{r})$ has the same periodicity of the lattice:

$$U(\mathbf{r} + \mathbf{R}) = U(\mathbf{r}), \quad (1.20)$$

where \mathbf{R} is a translation vector of the crystal, given by Eq. 1.1. We recall that in vacuum, where $U(\mathbf{r}) = 0$, the stationary wavefunctions of the free electrons in a volume V are given by:

$$\psi_{\mathbf{k}}(\mathbf{r}) = \frac{1}{\sqrt{V}} e^{i\mathbf{k}\cdot\mathbf{r}},$$

delocalized over all the space with uniform probability density, \mathbf{k} is the wavevector. The electron momentum and energy are given by the following expressions:

$$\mathbf{p} = \hbar\mathbf{k}, \quad \mathcal{E} = \frac{\hbar^2 k^2}{2m_0}, \quad (1.21)$$

where m_0 is the free electron mass. It is possible to demonstrate that the solutions of the Schrödinger equation for a periodic potential are *Bloch–Floquet* (or simply Bloch) *functions* so that (*Bloch's theorem*):

$$\psi_{n\mathbf{k}}(\mathbf{r}) = u_{n\mathbf{k}}(\mathbf{r}) e^{i\mathbf{k}\cdot\mathbf{r}}, \quad (1.22)$$

where $u_{n\mathbf{k}}(\mathbf{r})$ has the same periodicity of the crystal:

$$u_{n\mathbf{k}}(\mathbf{r} + \mathbf{R}) = u_{n\mathbf{k}}(\mathbf{r}), \quad (1.23)$$

\mathbf{k} is the wave vector, and n refers to the band (as will be discussed in this chapter). The Bloch functions are the product of a plane wave and a function $u_{n\mathbf{k}}(\mathbf{r})$, with the lattice periodicity. It is evident that the Bloch wavefunction is not periodic; indeed,

$$\psi_{n\mathbf{k}}(\mathbf{r} + \mathbf{R}) = \psi_{n\mathbf{k}}(\mathbf{r}) e^{i\mathbf{k}\cdot\mathbf{R}}, \quad (1.24)$$

while the electron probability density is periodic:

$$|\psi_{n\mathbf{k}}(\mathbf{r} + \mathbf{R})|^2 = |\psi_{n\mathbf{k}}(\mathbf{r})|^2. \quad (1.25)$$

1.3.1 Intuitive Proof of Bloch's Theorem in the Case of a Linear Lattice

Let us consider a linear lattice with lattice constant a . $U(x)$ is the periodic potential, such that $U(x + ma) = U(x)$, where m is an integer. We assume that the electron distribution has the same periodicity of the lattice, so that:

$$|\psi(x + ma)|^2 = |\psi(x)|^2. \quad (1.26)$$

Equation 1.26 implies that

$$\psi(x + ma) = C\psi(x), \quad (1.27)$$

where C is a quantity satisfying the condition $|C|^2 = 1$. Therefore, we may write $C = e^{ikma}$, where k is an arbitrary parameter. From Eq. 1.27, we obtain:

$$\psi(x) = e^{-ikma}\psi(x + ma). \quad (1.28)$$

Multiplying both sides of the previous equation by e^{-ikx} , we obtain

$$\psi(x)e^{-ikx} = e^{-ik(x+ma)}\psi(x + ma), \quad (1.29)$$

thus showing that the function $u(x) = e^{-ikx}\psi(x)$ is periodic with the period a . Finally, by writing $\psi(x) = e^{ikx}u(x)$, we obtain the expression of Bloch's theorem in the case of a linear lattice. ■

If \mathbf{G} is a translation vector in the reciprocal space, the Bloch function can be written as:

$$\psi_{n\mathbf{k}}(\mathbf{r}) = u_{n\mathbf{k}}(\mathbf{r}) e^{i\mathbf{k}\cdot\mathbf{r}} = [u_{n\mathbf{k}}(\mathbf{r})e^{-i\mathbf{G}\cdot\mathbf{r}}]e^{i(\mathbf{k}+\mathbf{G})\cdot\mathbf{r}}, \quad (1.30)$$

which is still a Bloch function since the function between the square brackets in the previous equation has the same periodicity as that of the lattice (see Eq. 1.11). Therefore, the wavefunction 1.30 is the solution of the Schrödinger equation (Eq. 1.19) for the wavevector $\mathbf{k} + \mathbf{G}$. We conclude that, for a given band n , the eigenstates, $\psi_{n\mathbf{k}}(\mathbf{r})$, and eigenvalues, $\mathcal{E}_n(\mathbf{k})$, are periodic functions of \mathbf{k} in the reciprocal lattice:

$$\psi_{n\mathbf{k}}(\mathbf{r}) = \psi_{n,\mathbf{k}+\mathbf{G}}(\mathbf{r}) \quad (1.31)$$

$$\mathcal{E}_n(\mathbf{k}) = \mathcal{E}_n(\mathbf{k} + \mathbf{G}). \quad (1.32)$$

These two important expressions clearly demonstrate that we can restrict our analysis to the first Brillouin zone. In particular, it is possible to represent the dispersion relation $\mathcal{E}_n(\mathbf{k})$ only in this zone by performing a translation of the outer branches into the first Brillouin zone by the reciprocal lattice wavevector \mathbf{G} , so that $\mathbf{k} + \mathbf{G}$ is contained in the first zone. This procedure is called band folding.

In order to calculate the dispersion relation $\mathcal{E}_n(\mathbf{k})$, which gives the relationship among electron energy in a crystal, the wavevectors \mathbf{k} in the first Brillouin zone and the band index n , one has to solve the Schrödinger equation obtained by introducing the Bloch wavefunctions 1.22 into Eq. 1.19. The set of curves $\mathcal{E}_n(\mathbf{k})$ defines the band structure of the material. The Bloch wavefunctions are labeled also with respect to the band index n since,

for a given value of \mathbf{k} , there are many solutions of the Schrödinger equation. Indeed, if we introduce the Bloch function in the Schrödinger equation, we obtain:

$$\left[\frac{\hbar^2}{2m} (-i\nabla + \mathbf{k})^2 + U(\mathbf{r}) \right] u_{n\mathbf{k}}(\mathbf{r}) = \mathcal{E}_n(\mathbf{k}) u_{n\mathbf{k}}(\mathbf{r}). \quad (1.33)$$

Therefore, $u_{n\mathbf{k}}(\mathbf{r})$ is determined by the eigenvalue problem

$$H_B u_{n\mathbf{k}}(\mathbf{r}) = \mathcal{E}_n(\mathbf{k}) u_{n\mathbf{k}}(\mathbf{r}), \quad (1.34)$$

where:

$$H_B = \frac{\hbar^2}{2m} (-i\nabla + \mathbf{k})^2 + U(\mathbf{r}), \quad (1.35)$$

with boundary conditions:

$$u_{n\mathbf{k}}(\mathbf{r}) = u_{n\mathbf{k}}(\mathbf{r} + \mathbf{R}). \quad (1.36)$$

Due to the periodic boundary conditions, this eigenvalue problem is restricted to a single primitive cell of the crystal, and an infinite set of solutions exists with discretely spaced eigenvalues, which can be labeled by the band index n . If we fix the value of n and vary \mathbf{k} in the first Brillouin zone, it is possible to obtain the dispersion curve $\mathcal{E}_n(\mathbf{k})$, which gives the n th energy band of the periodic structure.

1.3.1 Orthonormality of the Bloch Wavefunctions

The periodic functions $u_{n\mathbf{k}}(\mathbf{r})$ form a set of orthogonal wavefunctions since the operator H_B given by Eq. 1.35 is Hermitian. We can add a normalizing condition by writing:

$$\frac{1}{V_{uc}} \int_{uc} u_{m\mathbf{k}}^*(\mathbf{r}) u_{n\mathbf{k}}(\mathbf{r}) d\tau = \delta_{mn}, \quad (1.37)$$

where V_{uc} is the volume of the unit cell and δ_{mn} is the Kronecker delta. If we now consider the Bloch function associated with the n th band corresponding to a particular \mathbf{k} value, we can write the Bloch function in a slightly different way by requiring the normalization condition:

$$\int_V \psi_{n\mathbf{k}}^*(\mathbf{r}) \psi_{n\mathbf{k}}(\mathbf{r}) d\tau = 1, \quad (1.38)$$

where $V = NV_{uc}$ is the volume of the crystal (more precisely, as will be explained in Chapter 2, V is the volume of the periodic boxes in which a crystal can be divided). If we write:

$$\psi_{n\mathbf{k}}(\mathbf{r}) = A e^{i\mathbf{k}\cdot\mathbf{r}} u_{n\mathbf{k}}(\mathbf{r}), \quad (1.39)$$

and use this expression in Eq. 1.38, we obtain:

$$A = \frac{1}{\sqrt{NV_{uc}}} = \frac{1}{\sqrt{V}}, \quad (1.40)$$

so that the Bloch function can be written as:

$$\psi_{n\mathbf{k}}(\mathbf{r}) = \frac{1}{\sqrt{V}} e^{i\mathbf{k}\cdot\mathbf{r}} u_{n\mathbf{k}}(\mathbf{r}). \quad (1.41)$$

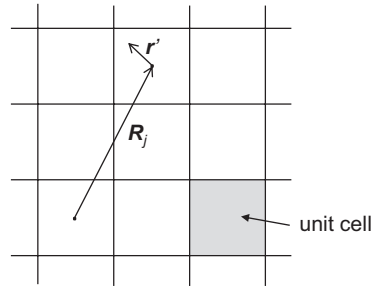


Figure 1.12

Transformation of the spatial coordinates used to calculate the integral Eq. 1.42. \mathbf{R}_j is the position vector of the j -th unit cell and \mathbf{r}' is confined within a single unit cell. A generic unit cell is shown as a gray square.

It is possible to demonstrate that the wavefunctions associated with different \mathbf{k} -values are orthogonal. The scalar product between two Bloch states with different \mathbf{k} is given by the following expression:

$$\int_V \psi_{m\mathbf{k}'}^*(\mathbf{r}) \psi_{n\mathbf{k}}(\mathbf{r}) d\tau = \frac{1}{V} \int_V e^{-i\mathbf{k}' \cdot \mathbf{r}} u_{m\mathbf{k}'}^*(\mathbf{r}) e^{i\mathbf{k} \cdot \mathbf{r}} u_{n\mathbf{k}}(\mathbf{r}) d\tau. \quad (1.42)$$

We can first calculate the integral over a single unit cell and then sum the result considering all the unit cells in the crystal volume V . In order to use this approach, we first replace the spatial coordinate \mathbf{r} with a new spatial coordinate:

$$\mathbf{r} \rightarrow \mathbf{r}' + \mathbf{R}_j, \quad (1.43)$$

where \mathbf{R}_j is the position vector of the j -th unit cell and \mathbf{r}' is confined within a single unit cell, as schematically displayed in Fig. 1.12. Since $u_{n\mathbf{k}}(\mathbf{r})$ is periodic, we have:

$$u_{n\mathbf{k}}(\mathbf{r}' + \mathbf{R}_j) = u_{n\mathbf{k}}(\mathbf{r}'). \quad (1.44)$$

The scalar product 1.42 can be written as:

$$\sum_{j=1}^N \left[\frac{1}{V} e^{i(\mathbf{k}-\mathbf{k}') \cdot \mathbf{R}_j} \int_{V_j} e^{i(\mathbf{k}-\mathbf{k}') \cdot \mathbf{r}'} u_{m\mathbf{k}'}^*(\mathbf{r}') u_{n\mathbf{k}}(\mathbf{r}') d\tau \right], \quad (1.45)$$

where V_j is the volume of the j -th unit cell. Since the integral over the unit cell is the same for each unit cell, it can be extracted from the sum:

$$\left(\sum_{j=1}^N e^{i(\mathbf{k}-\mathbf{k}') \cdot \mathbf{R}_j} \right) \frac{1}{V} \int_{V_j} e^{i(\mathbf{k}-\mathbf{k}') \cdot \mathbf{r}'} u_{m\mathbf{k}'}^*(\mathbf{r}') u_{n\mathbf{k}}(\mathbf{r}') d\tau. \quad (1.46)$$

The term within parentheses is different from zero only if $\mathbf{k} = \mathbf{k}'$ and can be written as:

$$\sum_{j=1}^N e^{i(\mathbf{k}-\mathbf{k}') \cdot \mathbf{R}_j} = N \delta_{\mathbf{k}, \mathbf{k}'}, \quad (1.47)$$

where $\delta_{\mathbf{k}, \mathbf{k}'}$ is the Kronecker delta. Therefore, the scalar product 1.42 can be written as:

$$\int_V \psi_{m\mathbf{k}'}^*(\mathbf{r}) \psi_{n\mathbf{k}}(\mathbf{r}) d\tau = \delta_{\mathbf{k}, \mathbf{k}'} \delta_{mn}. \quad (1.48)$$

Note that the Bloch functions $\psi_{n\mathbf{k}}(\mathbf{r})$, characterized by different \mathbf{k} -values, are orthogonal. This property does not hold in the case of the periodic functions $u_{n\mathbf{k}}(\mathbf{r})$.

1.3.2 Momentum of an Electron in a Periodic Crystal

We note that the vector \mathbf{k} used in the previous equations plays the same role of the wavevector \mathbf{k} in the case of a free electron. However, there is an important difference: While for free electrons, the momentum can be written as $\mathbf{p} = \hbar\mathbf{k}$, in the case of electrons in a periodic structure $\hbar\mathbf{k}$ is not the electron momentum. Indeed, it can be easily demonstrated that the Bloch wavefunction $\psi_{n\mathbf{k}}$ is not an eigenstate of the momentum operator $\mathbf{p} = -i\hbar\nabla$. In fact, if we apply the momentum operator to a Bloch function, we obtain:

$$-i\hbar\nabla\psi_{n\mathbf{k}} = -i\hbar\nabla(u_{n\mathbf{k}}(\mathbf{r})e^{i\mathbf{k}\cdot\mathbf{r}}) = \hbar\mathbf{k}\psi_{n\mathbf{k}} - i\hbar e^{i\mathbf{k}\cdot\mathbf{r}}\nabla u_{n\mathbf{k}}(\mathbf{r}). \quad (1.49)$$

In contrast, in the case of a free electron, the application of the momentum operator leads to the following equation:

$$-i\hbar\nabla\psi_{\mathbf{k}} = \hbar\mathbf{k}\psi_{\mathbf{k}}, \quad (1.50)$$

thus showing that the wave function $\psi_{\mathbf{k}}$ is an eigenfunction of the momentum operator with the eigenvalue $\hbar\mathbf{k}$. The velocity of the electron with wavevector \mathbf{k} is therefore given by $\mathbf{v} = \hbar\mathbf{k}/m$.

The physical meaning of the term $\hbar\mathbf{k}$, associated with an electron in a crystal and called *crystal momentum*, can be understood by considering the equation of motion of an electron in a periodic structure and under the action of an externally applied electromagnetic field. To study the motion of an electron in a particular band, from the quantum-mechanical point of view we have to consider the wave packet formed by wavefunctions characterized by wavenumbers \mathbf{k}' distributed around a particular \mathbf{k} value:

$$\begin{aligned} \phi_{n\mathbf{k}}(\mathbf{r}, t) &= \sum_{\mathbf{k}'} g(\mathbf{k}') u_{n\mathbf{k}'}(\mathbf{r}) e^{i(\mathbf{k}'\cdot\mathbf{r} - \omega_n t)} = \\ &= \sum_{\mathbf{k}'} g(\mathbf{k}') \psi_{n\mathbf{k}'}(\mathbf{r}) \exp\left(-i\frac{\mathcal{E}_n(\mathbf{k}')}{\hbar}t\right), \end{aligned} \quad (1.51)$$

where we have written $\omega_n = \mathcal{E}_n/\hbar$. It is assumed that the \mathbf{k}' values are within an interval around \mathbf{k} much smaller than the extension of the Brillouin zone. The group velocity of the wave packet is:

$$\mathbf{v}_{gn} = \frac{\partial\omega_n}{\partial\mathbf{k}} = \frac{1}{\hbar} \frac{\partial\mathcal{E}_n(\mathbf{k})}{\partial\mathbf{k}}, \quad (1.52)$$

which can also be written as:

$$\mathbf{v}_{gn} = \frac{1}{\hbar} \nabla_{\mathbf{k}} \mathcal{E}_n(\mathbf{k}), \quad (1.53)$$

where:

$$\nabla_{\mathbf{k}} \equiv \frac{\partial}{\partial k_x} \mathbf{u}_x + \frac{\partial}{\partial k_y} \mathbf{u}_y + \frac{\partial}{\partial k_z} \mathbf{u}_z. \quad (1.54)$$

The dispersion relation $\mathcal{E}_n(\mathbf{k})$ contains all the effects of the crystal on the motion of the electron. If \mathbf{E} is the applied electric field, the work done by \mathbf{E} on the electron (charge $-e$) during the time interval dt is:

$$d\mathcal{E} = -e\mathbf{E} \cdot d\mathbf{r} = -e\mathbf{E} \cdot \mathbf{v}_g dt = -e\mathbf{E} \cdot \frac{1}{\hbar} \frac{d\mathcal{E}}{d\mathbf{k}} dt. \quad (1.55)$$

Therefore, we obtain:

$$\frac{d(\hbar\mathbf{k})}{dt} = -e\mathbf{E} = \mathbf{F}_{ext}, \quad (1.56)$$

where $\mathbf{F}_{ext} = -e\mathbf{E}$ is the external force acting on the electron. Upon considering also the effects of the magnetic field, Eq. 1.56 can be written as:

$$\frac{d(\hbar\mathbf{k})}{dt} = -e[\mathbf{E}(\mathbf{r}, t) + \mathbf{v}_g(\mathbf{k}) \times \mathbf{B}(\mathbf{r}, t)]. \quad (1.57)$$

While in the case of free electrons $-e\mathbf{E}$ (or $-e(\mathbf{E} + \mathbf{v}_g \times \mathbf{B})$) is the total force acting on the charged particles (and therefore from Eqs. 1.56 and 1.57, we obtain that $\hbar\mathbf{k}$ is the electron momentum), for an electron in a crystal $-e\mathbf{E}$ represents only the external force, while the total force is given by $\mathbf{F}_{ext} + \mathbf{F}_{int}$, where \mathbf{F}_{int} represents the resultant internal force from the crystal lattice. Therefore:

$$\frac{d\mathbf{p}}{dt} = \mathbf{F}_{ext} + \mathbf{F}_{int}. \quad (1.58)$$

1.4 The Concept of Effective Mass

In the case of free electrons, the energy is given by Eq. 1.21, so that the electron mass can be written as:

$$\frac{1}{m_0} = \frac{1}{\hbar^2} \frac{d^2\mathcal{E}}{dk^2}. \quad (1.59)$$

This expression can be generalized for an arbitrary dispersion relation $\mathcal{E}(\mathbf{k})$. If we differentiate Eq. 1.52, we obtain:

$$\frac{dv_{gn}}{dt} = \frac{1}{\hbar} \frac{\partial^2 \mathcal{E}_n}{\partial t \partial k} = \frac{1}{\hbar} \frac{\partial^2 \mathcal{E}_n}{\partial k^2} \frac{\partial k}{\partial t}. \quad (1.60)$$

By using Eq. 1.56, we have:

$$\frac{dv_{gn}}{dt} = \left(\frac{1}{\hbar^2} \frac{\partial^2 \mathcal{E}_n}{\partial k^2} \right) F_{ext}, \quad \text{or} \quad F_{ext} = \frac{\hbar^2}{\partial^2 \mathcal{E}_n / \partial k^2} \frac{dv_{gn}}{dt}. \quad (1.61)$$

Comparing Eq. 1.61 with Newton's second law, we obtain the definition of the *effective mass* m^* :

$$\frac{1}{m^*} = \frac{1}{\hbar^2} \frac{\partial^2 \mathcal{E}_n}{\partial k^2}. \quad (1.62)$$

The previous equation can be generalized to take into account an anisotropic energy surface (this is the case with important semiconductors such as Si and Ge). Since the effective mass is generally dependent on direction, it is a tensor.

If we differentiate both sides of Eq. 1.53 with respect to time, we have:

$$\frac{d\mathbf{v}_{gn}}{dt} = \frac{d}{dt} \left(\frac{1}{\hbar} \nabla_{\mathbf{k}} \mathcal{E}_n \right) = \frac{1}{\hbar} \nabla_{\mathbf{k}} \left(\frac{d\mathcal{E}_n}{dt} \right) = \frac{1}{\hbar} \nabla_{\mathbf{k}} \left(\frac{d\mathbf{k}}{dt} \cdot \nabla_{\mathbf{k}} \mathcal{E}_n \right). \quad (1.63)$$

By using Eq. 1.56 in the previous expression, we obtain:

$$\frac{d\mathbf{v}_{gn}}{dt} = \frac{1}{\hbar^2} \nabla_{\mathbf{k}} (\mathbf{F}_{ext} \cdot \nabla_{\mathbf{k}} \mathcal{E}_n), \quad (1.64)$$

where:

$$\mathbf{F}_{ext} \cdot \nabla_{\mathbf{k}} \mathcal{E}_n = F_{ext,x} \frac{\partial \mathcal{E}_n}{\partial k_x} + F_{ext,y} \frac{\partial \mathcal{E}_n}{\partial k_y} + F_{ext,z} \frac{\partial \mathcal{E}_n}{\partial k_z}, \quad (1.65)$$

so that:

$$\begin{aligned} \frac{d\mathbf{v}_{gn}}{dt} &= \frac{1}{\hbar^2} \left[F_{ext,x} \frac{\partial^2 \mathcal{E}_{n\mathbf{k}}}{\partial k_x^2} + F_{ext,y} \frac{\partial^2 \mathcal{E}_{n\mathbf{k}}}{\partial k_x \partial k_y} + F_{ext,z} \frac{\partial^2 \mathcal{E}_{n\mathbf{k}}}{\partial k_x \partial k_z} \right] \mathbf{u}_x + \\ &= \frac{1}{\hbar^2} \left[F_{ext,x} \frac{\partial^2 \mathcal{E}_{n\mathbf{k}}}{\partial k_y \partial k_x} + F_{ext,y} \frac{\partial^2 \mathcal{E}_{n\mathbf{k}}}{\partial k_y^2} + F_{ext,z} \frac{\partial^2 \mathcal{E}_{n\mathbf{k}}}{\partial k_y \partial k_z} \right] \mathbf{u}_y + \\ &= \frac{1}{\hbar^2} \left[F_{ext,x} \frac{\partial^2 \mathcal{E}_{n\mathbf{k}}}{\partial k_z \partial k_x} + F_{ext,y} \frac{\partial^2 \mathcal{E}_{n\mathbf{k}}}{\partial k_z \partial k_y} + F_{ext,z} \frac{\partial^2 \mathcal{E}_{n\mathbf{k}}}{\partial k_z^2} \right] \mathbf{u}_z. \end{aligned} \quad (1.66)$$

From the previous equation, we obtain a simple expression for a given component of the temporal derivative of the group velocity:

$$\left(\frac{d\mathbf{v}_{gn}}{dt} \right)_i = \frac{1}{\hbar^2} \frac{\partial^2 \mathcal{E}_{n\mathbf{k}}}{\partial k_i \partial k_j} F_{ext,j}, \quad (1.67)$$

where i and j refer to the x , y , and z coordinates and the right-hand side of the previous equation is summed over the double subscript. Equation 1.66 can be written in a very simple form by using the concept of effective mass, m^* :

$$\frac{d\mathbf{v}_{gn}}{dt} = \frac{1}{m^*} \mathbf{F}_{ext}, \quad (1.68)$$

where $1/m^*$ is a second-rank symmetric tensor, whose elements are:

$$\frac{1}{m_{ij}^*} = \frac{1}{\hbar^2} \frac{\partial^2 \mathcal{E}_{n\mathbf{k}}}{\partial k_i \partial k_j}. \quad (1.69)$$

A symmetric second-rank tensor can always be diagonalized by a proper axis rotation: The directions for which the matrix is diagonal are called the principal axis. In general, the values of the effective mass along each of the three principal axes are different.

1.5 Energy Bands

It is well known that, in atoms, bound electrons occupy discrete energy levels; in solids, such discrete levels broaden to form allowed bands, which can be separated by band gaps, as shown in Fig. 1.13. Indeed, when the distance between two initially isolated atoms

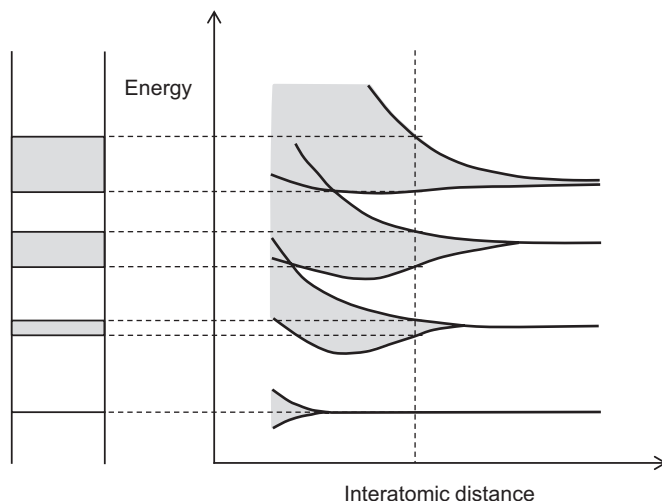


Figure 1.13 Formation of energy bands.

is decreased, their electronic orbitals overlap and the final wavefunction is described by two combinations, $\psi_1 \pm \psi_2$, of the two atomic wavefunctions, which correspond to the bonding and antibonding states of the final diatomic molecule. In the case of N atoms, N different orbitals are generated from each orbital of the isolated atom. In a given crystal lattice, there are several energy bands, which correspond to the atomic energy levels of the atoms composing the crystal, as schematically shown in Fig. 1.13, and the width of the band is proportional to the strength of the overlap interaction between neighboring atoms. The energy bands that derive from inner atomic shells are completely filled by electrons, which are more or less localized. In general, many important physical properties of the crystal are determined by electrons contained in bands, corresponding to the uppermost atomic shells, occupied by the valence electrons. If the uppermost band is not completely filled by electrons at 0 K, it is called the conduction band. If it is completely filled at 0 K, it is called the valence band and the empty band just above it is called the conduction band. The material in which the uppermost band is not completely filled is a metal, while in the second case, we have an insulator or a semiconductor, depending on the width of the energy gap, \mathcal{E}_g , between the valence and the conduction bands. As a rule of thumb, we have a semiconductor when $0 < \mathcal{E}_g \leq 4$ eV and an insulator when $\mathcal{E}_g > 4$ eV. This discrimination is not so sharp: Indeed, diamond, with an energy gap $\mathcal{E}_g = 5.5$ eV, is still considered a semiconductor. The materials with $\mathcal{E}_g = 0$ are called semimetals. When a band is completely filled by electrons, such electrons cannot conduct any current.

1.5.1 Electrons and Holes in a Semiconductor

In the case of a semiconductor, upon increasing the temperature, some electrons can be excited from the valence to the conduction band. In this way, the valence band is left with a few empty states. Empty states in a band are generally called holes. When an external

electromagnetic field is applied to a semiconductor, a hole behaves as a particle with a positive charge e . Let us consider a completely filled band. In this case, the sum of all the wave vectors of the electrons is zero:

$$\sum \mathbf{k} = 0, \quad (1.70)$$

the sum being over all states of the considered band in the first Brillouin zone. This is a consequence of the inversion symmetry of the first Brillouin zone, which follows from the symmetry under the inversion $\mathbf{r} \rightarrow -\mathbf{r}$ about any lattice point of the crystal lattice. As a result, there is the same number of filled states with positive wavenumber \mathbf{k} and with negative wavenumber $-\mathbf{k}$. If an electron with wavenumber \mathbf{k}_e is promoted from the valence to the conduction band, the total wavevector is now $\sum \mathbf{k} = -\mathbf{k}_e$. This wavevector is assigned to the hole, so that the wavevector of the hole, \mathbf{k}_h , is given by:

$$\mathbf{k}_h = -\mathbf{k}_e. \quad (1.71)$$

The equation of motion of the missing electron in an electromagnetic field is given by Eq. 1.57:

$$\frac{d(\hbar\mathbf{k}_e)}{dt} = -e(\mathbf{E} + \mathbf{v}_g \times \mathbf{B}). \quad (1.72)$$

Therefore, the corresponding equation of motion of the hole (with $\mathbf{k}_h = -\mathbf{k}_e$) is:

$$\frac{d(\hbar\mathbf{k}_h)}{dt} = e(\mathbf{E} + \mathbf{v}_g \times \mathbf{B}), \quad (1.73)$$

which is the equation of motion of a particle with positive charge e .

1.6 Calculation of the Band Structure

Various techniques can be employed to calculate the dependence of energy versus wavevector, that is the dispersion relation $\mathcal{E}(\mathbf{k})$, which gives the band structure of the material. It is not the aim of this section to describe in detail these band structure calculations, which are extensively treated in many textbooks. Each method must solve two main problems: (i) the determination of the periodic one-electron potential, $U(\mathbf{r})$, of the crystal, which is contained in the Schrödinger equation; (ii) find the eigenvalues and eigenfunctions of this equation. The various methods differ in the procedures used to solve these two problems. In the following, the tight-binding method (TBM) will be briefly discussed, mainly for didactic reasons, since, in particular situations, it allows one to derive analytic expressions for the dispersion relation $\mathcal{E}(\mathbf{k})$, which are very useful to get a simple physical understanding of the band structure. We will also mention the so-called $\mathbf{k} \cdot \mathbf{p}$ method. Many other methods can be employed: for example, the pseudopotential method, the cellular (Wigner–Seitz) method, the so-called muffin-tin methods, which include the augmented plane wave (APW) method, and others.

1.6.1 Tight-Binding Method

TBM is an empirical approach since experimental inputs have to be used to fit the actual band structure. In the previous section, we saw how energy bands are created upon progressively reducing the distances between the atoms composing the crystal. In the final configuration, the atomic wavefunctions of neighboring atoms can be more or less overlapped: The TBM can be properly applied when the overlap of the atomic wavefunctions cannot be neglected, but it is not too large, so that the atomic description can still be used. In this case, the atomic wavefunctions can be used as a basis set for the Bloch functions. Strictly speaking, in order to obtain the eigenstates of the valence electrons of a crystal, all atomic wavefunctions of the atoms composing the crystal are required, since only all atomic orbitals compose a complete basis set. However, the largest contribution is given by the atomic orbitals of the valence shells of the free atoms: Within the TBM, only these orbitals are considered. For example, for the elemental semiconductors of group IV of the periodic table, the valence shell orbitals are formed by the $2s$ and $2p$ states in the case of C, by the $3s$ and $3p$ states for Si, and by the $4s$ and $4p$ states for Ge. In the case of semiconductors formed by different elements, the valence shell orbitals of the various atoms have to be considered. For example, in the case of GaAs, the $4s$ state and the $4p$ states of Ga and the $4s$ and $4p$ states of As must be considered. In the above examples, the valence shells of the atoms are formed by s -type or p -type orbitals.

We will assume a lattice with a single atom basis. We will further assume that the bound states of the atomic Hamiltonian, H_{at} , are well localized so that the wavefunction $\psi_n(\mathbf{r})$ for an atom placed at the origin ($\mathbf{r} = 0$) becomes very small at a distance from the origin of the order of the lattice constant. $\psi_n(\mathbf{r})$ is given by:

$$H_{at}\psi_n = \mathcal{E}_n\psi_n. \quad (1.74)$$

We assume that close to each lattice point the crystal Hamiltonian, H , can be approximated by H_{at} . The crystal Hamiltonian can be written as:

$$H = H_{at} + \Delta U(\mathbf{r}), \quad (1.75)$$

where $\Delta U(\mathbf{r})$ is the correction to the atomic potential, which has to be added to obtain the periodic potential of the crystal, as shown schematically in Fig. 1.14. If $\Delta U(\mathbf{r})$ vanishes in the region where the atomic orbital $\psi_n(\mathbf{r})$ is localized ($\mathbf{r} = 0$ in Fig. 1.14), $\psi_n(\mathbf{r})$ will also be a solution of the Schrödinger equation with the Hamiltonian given by Eq. 1.75. In this case, the crystal wavefunction $\psi_{\mathbf{k}}(\mathbf{r})$ can be written as a linear combination of atomic wavefunctions. Since $\psi(\mathbf{r})$ must satisfy the Bloch condition:

$$\psi_{\mathbf{k}}(\mathbf{r} + \mathbf{R}_0) = e^{i\mathbf{k}\cdot\mathbf{R}_0}\psi_{\mathbf{k}}(\mathbf{r}), \quad (1.76)$$

the linear combination can be written as follows:

$$\psi_{\mathbf{k}}(\mathbf{r}) = \sum_{\mathbf{R}} e^{i\mathbf{k}\cdot\mathbf{R}}\psi_n(\mathbf{r} - \mathbf{R}), \quad (1.77)$$

where the wavevector \mathbf{k} varies within the first Brillouin zone and the sum over \mathbf{R} spans all the crystal lattice. This wavefunction satisfies the requirement of a Bloch wavefunction, indeed, considering a generic lattice vector \mathbf{R}_0 :

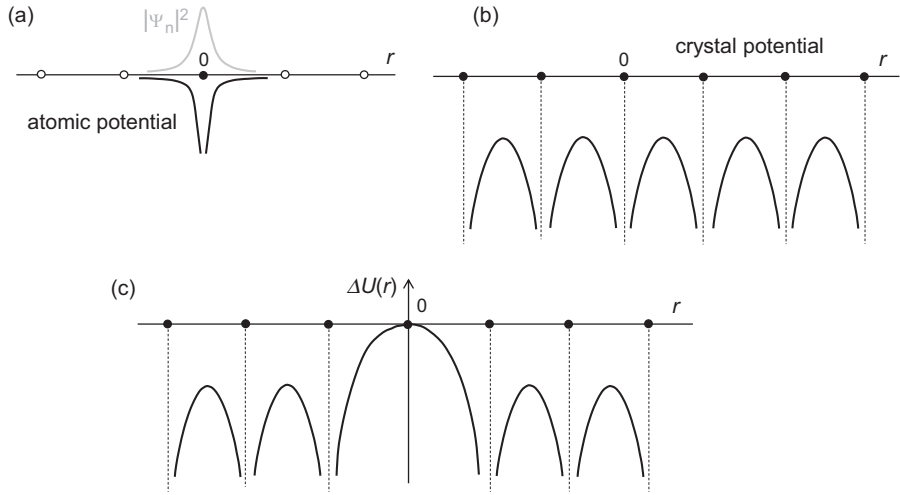


Figure 1.14

(a) Atomic potential of a single atom (black curve), the gray curve schematically represents the squared modulus of an atomic wavefunction, $|\psi_n|^2$, localized at the origin ($r = 0$). (b) Periodic crystal potential. (c) $\Delta U(\mathbf{r})$: correction to the atomic potential to obtain the periodic crystal potential.

$$\begin{aligned}\psi_{\mathbf{k}}(\mathbf{r} + \mathbf{R}_0) &= \sum_{\mathbf{R}} e^{i\mathbf{k}\cdot\mathbf{R}} \psi_n(\mathbf{r} - \mathbf{R} + \mathbf{R}_0) = \\ &= e^{i\mathbf{k}\cdot\mathbf{R}_0} \sum_{\mathbf{R}} e^{i\mathbf{k}\cdot(\mathbf{R}-\mathbf{R}_0)} \psi_n[\mathbf{r} - (\mathbf{R} - \mathbf{R}_0)].\end{aligned}\quad (1.78)$$

$\mathbf{R} - \mathbf{R}_0$ is simply another crystal translation vector, and since the sum over \mathbf{R} spans all the crystal, we can replace it by another translation vector, \mathbf{R}' , so that:

$$\psi_{\mathbf{k}}(\mathbf{r} + \mathbf{R}_0) = e^{i\mathbf{k}\cdot\mathbf{R}_0} \sum_{\mathbf{R}'} e^{i\mathbf{k}\cdot\mathbf{R}'} \psi_n(\mathbf{r} - \mathbf{R}') = e^{i\mathbf{k}\cdot\mathbf{R}_0} \psi_{\mathbf{k}}(\mathbf{r}).\quad (1.79)$$

It is evident that the energy $\mathcal{E}(\mathbf{k})$ associated with the wavefunction Eq. 1.77 is simply the energy of the atomic level, \mathcal{E}_n . This is related to our initial assumption of a $\Delta U(\mathbf{r})$ term which vanishes where $\psi_n(\mathbf{r})$ is localized: This assumption is not realistic. Instead, we have to assume that $\Delta U(\mathbf{r})$ is small but not precisely zero where $\psi_n(\mathbf{r})$ becomes small, so that the product $\Delta U(\mathbf{r})\psi_n(\mathbf{r})$ is very small but not zero. Therefore, a more realistic solution for the crystal Schrödinger equation, still satisfying the Bloch conditions, can be written as:

$$\psi(\mathbf{r}) = \sum_{\mathbf{R}} e^{i\mathbf{k}\cdot\mathbf{R}} \phi(\mathbf{r} - \mathbf{R}),\quad (1.80)$$

where $\phi(\mathbf{r})$ is very close, but not exactly equal, to the atomic wavefunction $\psi_n(\mathbf{r})$. We can assume that $\phi(\mathbf{r})$ can be written as a linear combination of a small number of localized atomic wavefunctions:

$$\phi(\mathbf{r}) = \sum_n b_n \psi_n(\mathbf{r}).\quad (1.81)$$

For this reason, the TBM is also known as the *linear combination of atomic orbitals (LCAO) method*.

The Schrödinger equation is now:

$$H\psi(\mathbf{r}) = [H_{at} + \Delta U(\mathbf{r})]\psi(\mathbf{r}) = \mathcal{E}(\mathbf{k})\psi(\mathbf{r}). \quad (1.82)$$

We then multiply this equation by the atomic wave function $\psi_m^*(\mathbf{r})$, integrate over all \mathbf{r} , and use the fact that:

$$\int \psi_m^*(\mathbf{r})H_{at}\psi(\mathbf{r})d\mathbf{r} = \int (H_{at}\psi_m(\mathbf{r}))^*\psi(\mathbf{r})d\mathbf{r} = \mathcal{E}_m \int \psi_m^*(\mathbf{r})\psi(\mathbf{r})d\mathbf{r}. \quad (1.83)$$

We obtain:

$$\mathcal{E}_m \int \psi_m^*(\mathbf{r})\psi(\mathbf{r})d\mathbf{r} + \int \psi_m^*(\mathbf{r})\Delta U(\mathbf{r})\psi(\mathbf{r})d\mathbf{r} = \mathcal{E}(\mathbf{k}) \int \psi_m^*(\mathbf{r})\psi(\mathbf{r})d\mathbf{r}, \quad (1.84)$$

which can be rewritten as:

$$[\mathcal{E}(\mathbf{k}) - \mathcal{E}_m] \int \psi_m^*(\mathbf{r})\psi(\mathbf{r})d\mathbf{r} = \int \psi_m^*(\mathbf{r})\Delta U(\mathbf{r})\psi(\mathbf{r})d\mathbf{r}. \quad (1.85)$$

Placing Eqs. 1.80–1.81 into Eq. 1.85 and using the orthonormality of the atomic wave functions:

$$\int \psi_m^*(\mathbf{r})\psi_n(\mathbf{r})d\mathbf{r} = \delta_{mn}. \quad (1.86)$$

We can write an eigenvalue equation from which it is possible to obtain the coefficients b_n and the Bloch energies $\mathcal{E}(\mathbf{k})$. In the sum over \mathbf{R} we separate the terms with $\mathbf{R} = 0$ and $\mathbf{R} \neq 0$:

$$\begin{aligned} [\mathcal{E}(\mathbf{k}) - \mathcal{E}_m]b_m &= -[\mathcal{E}(\mathbf{k}) - \mathcal{E}_m] \sum_n \left(\sum_{\mathbf{R} \neq 0} \int \psi_m^*(\mathbf{r})\psi_n(\mathbf{r} - \mathbf{R})e^{i\mathbf{k} \cdot \mathbf{R}}d\mathbf{r} \right) b_n + \\ &+ \sum_n \left(\int \psi_m^*(\mathbf{r})\Delta U(\mathbf{r})\psi_n(\mathbf{r})d\mathbf{r} \right) b_n + \\ &+ \sum_n \left(\sum_{\mathbf{R} \neq 0} \int \psi_m^*(\mathbf{r})\Delta U(\mathbf{r})\psi_n(\mathbf{r} - \mathbf{R})e^{i\mathbf{k} \cdot \mathbf{R}}d\mathbf{r} \right) b_n. \end{aligned} \quad (1.87)$$

In a semiconductor, we have to consider the valence shell of the atoms from which the crystal is formed; therefore, we need to consider an s -level and triply degenerate p -levels. For this reason, Eq. 1.87 gives rise to a set of four homogeneous equations, whose eigenvalues give the dispersion relations $\mathcal{E}(\mathbf{k})$ for the s -band and the three p -bands and whose solutions $b(\mathbf{k})$ give the amplitudes of the LCAO (see Eq. 1.81) forming the wavefunction $\phi(\mathbf{r})$ in the first Brillouin zone. In this case, we have to solve a 4×4 secular problem. The calculations are rather complex. To get some physical insight into the problem, we will solve a simple problem of one atom basis with only an s -function.

1.6.2 Crystal with One-Atom Basis and Single Atomic Orbital

Since we have to consider only one atomic level, the coefficients $\{b_m\}$ are zero except for the s -level, where $b_s = 1$. A single equation results in this case. If \mathcal{E}_s is the energy of the atomic s -level and we write $\psi_s(\mathbf{r}) = \phi(\mathbf{r})$, the following functions can be introduced:

$$\alpha(\mathbf{R}) = \int \phi^*(\mathbf{r})\phi(\mathbf{r} - \mathbf{R})d\mathbf{r} \quad (1.88)$$

$$\beta = - \int \phi^*(\mathbf{r})\Delta U(\mathbf{r})\phi(\mathbf{r})d\mathbf{r} = - \int \Delta U(\mathbf{r})|\phi(\mathbf{r})|^2d\mathbf{r} \quad (1.89)$$

$$\gamma(\mathbf{R}) = - \int \phi^*(\mathbf{r})\Delta U(\mathbf{r})\phi(\mathbf{r} - \mathbf{R})d\mathbf{r}. \quad (1.90)$$

Equation 1.87 can be rewritten in terms of the previous quantities:

$$\mathcal{E}(\mathbf{k}) = \mathcal{E}_s - \frac{\beta + \sum \gamma(\mathbf{R})e^{i\mathbf{k}\cdot\mathbf{R}}}{1 + \sum \alpha(\mathbf{R})e^{i\mathbf{k}\cdot\mathbf{R}}}. \quad (1.91)$$

Since we are considering an s -level, $\alpha(-\mathbf{R}) = \alpha(\mathbf{R})$, therefore given the fact that $\Delta U(-\mathbf{r}) = \Delta U(\mathbf{r})$, we also have that $\gamma(-\mathbf{R}) = \gamma(\mathbf{R})$. In Eq. 1.91, we can ignore the sum $\sum \alpha(\mathbf{R})e^{i\mathbf{k}\cdot\mathbf{R}}$ with respect to one since $\phi(\mathbf{r})$ is well localized so that the overlapping integral Eq. 1.88, which contains the product of two atomic wavefunctions centered on different sites, is very small. Moreover, we can make another simplifying assumption if we assume that in the sum $\sum \gamma(\mathbf{R})e^{i\mathbf{k}\cdot\mathbf{R}}$ we have to consider only the nearest neighbors (n.n.). Equation 1.91 can be written in a very simple form:

$$\mathcal{E}(\mathbf{k}) = \mathcal{E}_s - \beta - \sum_{\text{n.n.}} \gamma(\mathbf{R})e^{i\mathbf{k}\cdot\mathbf{R}}. \quad (1.92)$$

In the case of real semiconductors, we cannot limit ourself to considering a crystal with a one-atom basis and one atomic orbital. We have already observed that the outermost electrons are placed in four atomic orbitals (one s and three p orbitals, p_x , p_y , and p_z). Moreover, the corresponding lattice has a two-atom basis. In this case, the crystal states can be expanded as linear combinations of two Bloch states, corresponding to the two atoms of the basis. Therefore, by using Eqs. 1.80 and 1.81 we can write:

$$\psi(\mathbf{r}) = \sum_{\mathbf{R}} \sum_{m=1}^4 \sum_{j=1}^2 C_{mj}(\mathbf{k})\psi_{mj}(\mathbf{r} - \mathbf{r}_j - \mathbf{R})e^{i\mathbf{k}\cdot\mathbf{R}}, \quad (1.93)$$

where the index m refers to the different atomic orbitals (s , p_x , p_y , and p_z), the index j refers to the atom in the basis, and \mathbf{r}_j gives the position of the j -th atom in the unit cell. For example, in the case of the zinc-blende lattice (which is the structure of several semiconductors), for each atom of the two-atom basis we have an s orbital and three p orbitals, thus leading to a 8×8 secular problem (eight homogeneous equations of the form 1.87). Considering also the spin degeneracy, we would end up with a 16×16 secular problem, thus increasing the complexity of the tight-binding calculations.

In the following section, we will consider two very simple examples of lattices with a one-atom basis and a single atomic state (s -state) in order to see two simple applications of the TBM. These simple applications will allow us to discuss a few important physical properties, which can be generalized to more realistic situations.

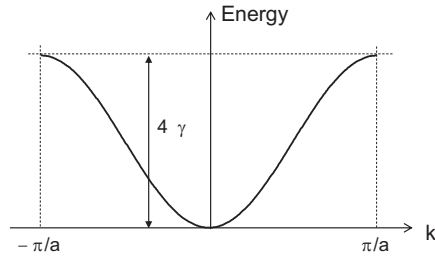


Figure 1.15 Dispersion relation, $\mathcal{E}(k)$, in the first Brillouin zone of a linear lattice.

1.6.3 Linear Lattice

In the case of a *linear lattice* with lattice constant a , the tight-binding wavefunction 1.80 can be written as:

$$\psi(x) = \sum_m e^{imka} \phi(x - ma). \quad (1.94)$$

From Eq. 1.92, we can immediately obtain the dispersion relation $\mathcal{E}(k)$ (which is shown in the first Brillouin zone in Fig. 1.15):

$$\mathcal{E}(k) = \mathcal{E}_s - \beta - \gamma(e^{ika} + e^{-ika}) = \mathcal{E}_s - \beta - 2\gamma \cos(ka). \quad (1.95)$$

The width of the band is 4γ , and it is proportional to the overlap integral. This is reasonable, since an increase of the overlap integral γ leads to a stronger interaction, and consequently a wider bandwidth. When the electron is near the bottom of the band, where $ka \ll 1$, we have:

$$\mathcal{E}(k) \simeq \mathcal{E}_s - \beta - 2\gamma \left(1 - \frac{1}{2}k^2 a^2\right) = \mathcal{E}_s - \beta - 2\gamma + \gamma k^2 a^2, \quad (1.96)$$

which has the same parabolic dependence on k as the dispersion relation of a free electron. Therefore, we may conclude that an electron in that region of the k -space behaves as a free electron with an effective mass:

$$m^* = \frac{\hbar^2}{2\gamma a^2}, \quad (1.97)$$

which shows that the effective mass is inversely proportional to the overlap integral γ . This is intuitively reasonable since if the overlap between atomic wavefunctions increases, it is easier for an electron to hop from one atomic site to another, thus leading to a reduction of its effective mass (less inertia for the electronic motion in the crystal).

Upon considering the other atomic energy levels, we end up with various energy bands, as shown in Figure 1.16(a). Figure 1.16(b) shows the resulting reduced zone scheme, which we discussed as a consequence of Eq. 1.32 (band-folding procedure). Upon using Eq. 1.95, it is possible to calculate the group velocity of the electron and the effective mass in the first Brillouin zone (not only around $k = 0$):

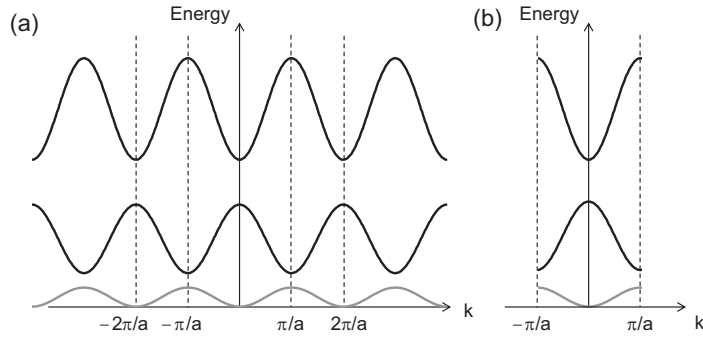


Figure 1.16 (a) Dispersion relation, $\mathcal{E}(k)$, in a linear lattice calculated by using the TBM. (b) Corresponding reduced zone scheme.

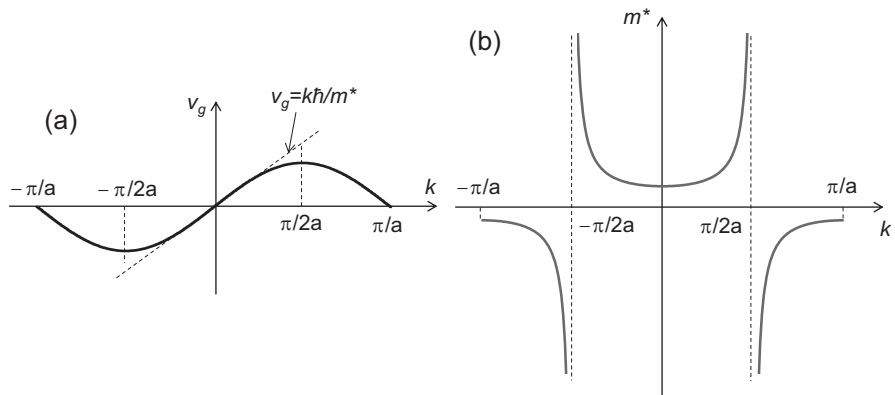


Figure 1.17 (a) Group velocity and (b) effective mass in the first Brillouin zone of a linear lattice.

$$v_g = \frac{1}{\hbar} \frac{\partial \mathcal{E}}{\partial k} = \frac{2\gamma a}{\hbar} \sin(ka), \tag{1.98}$$

$$m^* = \frac{\hbar^2}{\partial^2 \mathcal{E} / \partial k^2} = \frac{\hbar^2}{2\gamma a^2 \cos(ka)}. \tag{1.99}$$

Figure 1.17 shows v_g and m^* as a function of k . Note that in the central region of the first Brillouin zone, the group velocity is close to the free electron velocity, $\hbar k/m^*$. In this region, the electron can move almost freely through the lattice. This is no longer true approaching the borders of the Brillouin zone, $k = \pm\pi/a$: Here, the perturbation of the lattice is strong. This can be easily understood in terms of Bragg reflection in the linear lattice. Indeed, the Bragg condition for constructive interference of the waves scattered from each lattice point is $k = n\pi/a$. In this situation, we have a superposition between a forward ($k = \pi/a$) and a backward ($k = -\pi/a$) wave thus leading to a standing wave, which does not propagate in the crystal ($v_g = 0$).

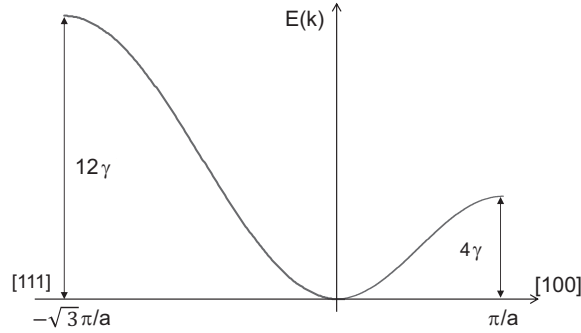


Figure 1.18 Dispersion curves along the [100] and [111] directions for a simple cubic lattice calculated by using the TBM.

1.6.4 Simple Cubic Lattice

Let us solve the problem for a simple cubic (sc) lattice. The six nearest neighbors are at:

$$\begin{aligned} &a(\pm 1, 0, 0) \\ &a(0, \pm 1, 0) \\ &a(0, 0, \pm 1). \end{aligned}$$

Equation 1.92 can be written as:

$$\begin{aligned} \mathcal{E}(\mathbf{k}) &= \mathcal{E}_s - \beta - \gamma(e^{ik_x a} + e^{-ik_x a} + e^{ik_y a} + e^{-ik_y a} + e^{ik_z a} + e^{-ik_z a}) \\ &= \mathcal{E}_s - \beta - 2\gamma(\cos k_x a + \cos k_y a + \cos k_z a). \end{aligned} \tag{1.100}$$

Along the [100] direction, we have ($k_x = k, k_y = k_z = 0$):

$$\mathcal{E}(\mathbf{k}) = \mathcal{E}_s - \beta - 2\gamma(\cos ka + 2). \tag{1.101}$$

The bottom of the band is at $k = 0$, and the bandwidth is 4γ . Along the [111] direction ($k_x^2 = k_y^2 = k_z^2 = k^2/3$), we have:

$$\mathcal{E}(\mathbf{k}) = \mathcal{E}_s - \beta - 6\gamma \cos \frac{ka}{\sqrt{3}}. \tag{1.102}$$

The bottom is at $k = 0$, and the bandwidth is 12γ . The top of the band is located at the extreme of the zone at $\sqrt{3}[\pi/a, \pi/a, \pi/a]$. The dispersion curves along the [100] and [111] directions are shown in Fig. 1.18. Also in this case, it is interesting to examine the band structure near the Γ point where $ka \ll 1$. Putting: $k_x^2 = k_y^2 = k_z^2 = k^2/3$, we have ($\cos x \simeq 1 - x^2/2$):

$$\begin{aligned} \mathcal{E}(\mathbf{k}) &= \mathcal{E}_s - \beta - 6\gamma \cos \frac{ka}{\sqrt{3}} \simeq \mathcal{E}_s - \beta - 6\gamma \left(1 - \frac{k^2 a^2}{6}\right) \\ &= \mathcal{E}_s - \beta - 6\gamma + \gamma k^2 a^2. \end{aligned} \tag{1.103}$$

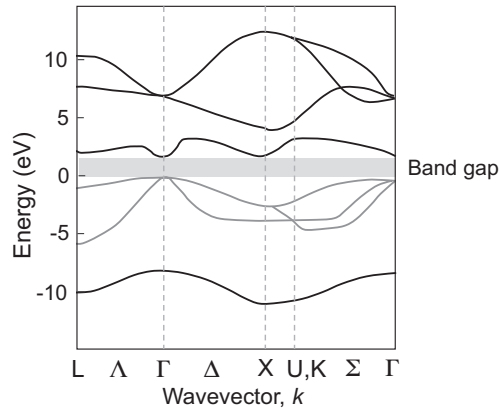


Figure 1.19 Calculated tight-binding band structure of GaAs without the effects of the spin–orbit coupling.

Comparing with the free electron problem solution, as in the previous example, we can obtain a simple expression for the effective mass (valid when $ka \ll 1$):

$$m^* = \frac{\hbar^2}{2\gamma a^2}. \quad (1.104)$$

1.6.5 Band Structure of Semiconductors Calculated by TBM

The band structure for GaAs calculated by using TBM is shown in Fig. 1.19. The top of the valence band and the bottom of the conduction band (referred to as the band edges of the semiconductor) are both at the Γ -point: GaAs is therefore a direct gap semiconductor. The states near the bottom of the conduction band have the symmetry of the s -state, whereas the states at the top of the valence band have the symmetry of the p -states. Generally, the states in the valence band can be written as linear combinations of p -orbitals. We note that the Bloch-lattice function maintains most of the symmetry properties as the original atomic orbitals. The band gap of the semiconductor and other properties in the high-symmetry points can be well fitted by using experimental inputs. Nevertheless, the calculated crystal structure shown in Fig. 1.19 does not reproduce the real structure of GaAs. This is clearly evident looking at the top of the valence band: Fig. 1.19 shows a threefold degeneracy, resulting from the degeneracy of the p_x , p_y , and p_z states. In contrast, measurements show that the top of the valence band is twofold degenerate and a third band is present below the valence band edge. This discrepancy is due to the fact that an important parameter has not been included so far in our discussion: the spin. The first result is to double the degeneracy of each state, both in the valence and conduction bands, without changing the dispersion curves. The second crucial effect is the spin–orbit interaction, which leads to changes of the energy curves in the valence band. Spin–orbit interaction is a relativistic effect: When an electron moves about the nucleus at relativistic velocity, the electric field generated by the nucleus Lorentz-transforms to a magnetic field, which interacts with the electron spin magnetic moment. In atoms, the spin–orbit interaction splits each electron energy level

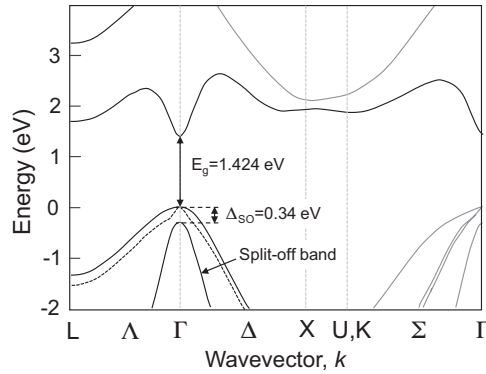


Figure 1.20

Calculated tight-binding band structure of GaAs including the effects of the spin-orbit coupling. Δ_{SO} is the spin-orbit splitting energy.

Table 1.2 Spin-orbit splitting energy for various semiconductors.

Semiconductor	Δ_{SO} (eV)
Si	0.044
Ge	0.29
GaAs	0.34
InAs	0.41
InSb	0.85

with a nonzero orbital quantum number ℓ . Spin-orbit splitting in the band structure of crystals is due to the same effect. Spin-orbit interaction leads to modifications in the valence band, whose states are primarily p -states. Without entering into any detail, spin-orbit interaction can be included in the tight-binding calculation by adding an additional term, H_{SO} , in the Hamiltonian:

$$H_{SO} = \xi \mathbf{L} \cdot \mathbf{S}, \quad (1.105)$$

where \mathbf{L} is the operator for orbital angular momentum, \mathbf{S} is the operator for spin angular momentum, and ξ can be treated as a constant. Upon considering the spin-orbit interaction, the dispersion curves calculated for GaAs modify as shown in Fig. 1.20. The top of the valence band loses part of its degeneracy: A *split-off band* is formed, separated by an energy offset Δ_{SO} from the top of the valence band. The spin-orbit splitting for various semiconductors are reported in Table 1.2.

The spin-orbit splitting energy Δ_{SO} of semiconductors increases as the fourth power of the atomic number of the constituent elements. Intuitively this can be understood as follows. If the atomic number Z (which gives the number of protons in the nucleus) increases, the electric field seen by the valence electrons also increases and consequently also the interaction between the orbital momentum and the spin. Δ_{SO} is small for materials composed of light atoms, as Si, and may be quite large in comparison with the energy gap in

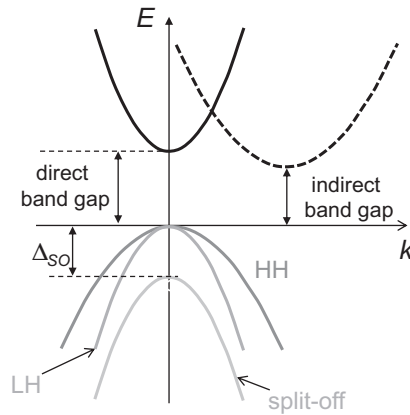


Figure 1.21 Schematic representation of the dispersion curves near the band edges of a semiconductor with direct or indirect (dashed conduction band curve) band gap. HH: heavy-hole valence band; LH: light-hole valence band.

semiconductors composed of heavy atoms, as InSb. Note that the conduction band is not affected by spin–orbit interaction (due to the s -symmetry) and remains doubly degenerate.

Figure 1.21 shows schematically the dispersion curves near the band edges of a semiconductor with direct or indirect (dashed conduction band curve) band gap. The doubly degenerate valence bands (fourfold degeneracy with spin) at the Γ -point are characterized by two different curvatures: These bands are called *heavy-hole* (HH) and *light-hole* (LH) bands. The band with the smaller curvature is the HH band, since the effective mass is inversely proportional to the band curvature.

So far we have considered only direct band gap semiconductors such as GaAs; there are semiconductors, like Si and Ge, where the k -value of the band edge of the conduction band is different from the k -value corresponding to the top of the valence band: These semiconductors are called *indirect*. For example, in Si the conduction band edge is close to the X -point and in Ge the conduction band edge is at the L -point, while for both semiconductors, the valence band edge is at the Γ -point. In the case of indirect semiconductors, the states at the conduction band edge present a strong anisotropy and can be described by combinations of s - and p -type states.

As will be clear in the following chapters, for most practical situations, only the dispersion relations close to the top of the valence band and to the bottom of the conduction bands have to be considered. For this reason, in most cases, parabolic dispersion relations can be considered. In this case, we can write:

$$\mathcal{E}(k) = \mathcal{E}_g + \frac{\hbar^2 k^2}{2m_c}, \quad (1.106)$$

in the conduction band, where \mathcal{E}_g is the energy gap and m_c is the effective mass in the conduction band, and

$$\mathcal{E}(k) = -\frac{\hbar^2 k^2}{2m_{lh}}, \quad \mathcal{E}(k) = -\frac{\hbar^2 k^2}{2m_{hh}}, \quad (1.107)$$

Table 1.3 Energy gap (in eV) and effective masses (in unit of the free electron mass m_0) of typical III–V semiconductors.

Material	\mathcal{E}_g (eV) (0 K)	\mathcal{E}_g (eV) (300 K)	m_c/m_0	m_{lh}/m_0	m_{hh}/m_0
GaAs	1.52	1.424	0.067	0.082	0.45
InP	1.42	1.27	0.08	0.089	0.6
InAs	0.43	0.354	0.023	0.025	0.41
InSb	0.23	0.17	0.014	0.016	0.40

in the valence band, where m_{lh} and m_{hh} are the effective masses for the LH and for the HH, respectively. Table 1.3 reports the values of the energy gap and effective masses for a few typical III–V semiconductors.

1.7 The $\mathbf{k} \cdot \mathbf{p}$ Method

In this section, we will briefly discuss another method, the $\mathbf{k} \cdot \mathbf{p}$ method, frequently used to calculate the band structure of semiconductors, which is quite accurate near the band edges. Here, we will just illustrate the basic idea at the heart of this method. In the following, we will use a few concepts and mathematical procedures which will be discussed in more detail in Chapter 3.

According to the Bloch theorem, the solution of the one-electron Schrödinger equation can be written as:

$$\psi_{n\mathbf{k}} = e^{i\mathbf{k}\cdot\mathbf{r}} u_{n\mathbf{k}}(\mathbf{r}), \quad (1.108)$$

where n is the band index, \mathbf{k} is the wvector in the first Brillouin zone, and $u_{n\mathbf{k}}(\mathbf{r})$ has the periodicity of the crystal. When Eq. 1.108 is substituted in the Schrödinger equation, the following equation in $u_{n\mathbf{k}}(\mathbf{r})$ is obtained:

$$\left(-\frac{\hbar^2}{2m_0} \nabla^2 - i \frac{\hbar \mathbf{k}}{m_0} \nabla + \frac{\hbar^2 k^2}{2m_0} + V(\mathbf{r}) \right) u_{n\mathbf{k}}(\mathbf{r}) = \mathcal{E}_{n\mathbf{k}} u_{n\mathbf{k}}(\mathbf{r}). \quad (1.109)$$

Since $\mathbf{p} = -i\hbar\nabla$, the previous equation can be written as:

$$\left(\frac{p^2}{2m_0} + \frac{\hbar \mathbf{k} \cdot \mathbf{p}}{m_0} + \frac{\hbar^2 k^2}{2m_0} + V \right) u_{n\mathbf{k}}(\mathbf{r}) = \mathcal{E}_{n\mathbf{k}} u_{n\mathbf{k}}(\mathbf{r}). \quad (1.110)$$

Therefore, the Hamiltonian can be written as the sum of two terms:

$$H = H_0 + H'_k, \quad (1.111)$$

where:

$$H_0 = \frac{p^2}{2m_0} + V \quad (1.112)$$

is the unperturbed Hamiltonian and

$$H'_k = \frac{\hbar \mathbf{k} \cdot \mathbf{p}}{m_0} + \frac{\hbar^2 k^2}{2m_0} \quad (1.113)$$

is the perturbation Hamiltonian. In the Γ -point ($\mathbf{k} = 0$) Eq. 1.110 gives:

$$\left(\frac{p^2}{2m_0} + V\right)u_{n0} = H_0u_{n0} = \mathcal{E}_{n0}u_{n0} \quad n = 1, 2, 3, \dots \quad (1.114)$$

The solutions of Eq. 1.114 form a complete and orthonormal set of basis functions. Now, we can use the terms $\hbar^2\mathbf{k} \cdot \mathbf{p}/m_0$ and $\hbar^2k^2/2m_0$ of the Hamiltonian as perturbations of the first and second order in \mathbf{k} . For this reason, the $\mathbf{k} \cdot \mathbf{p}$ model is quite accurate for small values of k . We note that the method can be used to calculate $\mathcal{E}_n(\mathbf{k})$ around any value \mathbf{k}_0 by expanding Eq. 1.110 around \mathbf{k}_0 if the wavefunctions and the energies at \mathbf{k}_0 are known. Now, if we assume that the band structure presents a stationary point (either a maximum or a minimum) at the energy \mathcal{E}_{n0} and that the band is nondegenerate at this energy, by using standard perturbation theory it is possible to show that the wavefunctions $u_{n\mathbf{k}}$ and the energies $\mathcal{E}_{n\mathbf{k}}$ can be written as:

$$u_{n\mathbf{k}} = u_{n0} + \frac{\hbar}{m_0} \sum_{n' \neq n} \frac{\langle u_{n0} | \mathbf{k} \cdot \mathbf{p} | u_{n'0} \rangle}{\mathcal{E}_{n0} - \mathcal{E}_{n'0}} u_{n'0} \quad (1.115)$$

$$\mathcal{E}_{n\mathbf{k}} = \mathcal{E}_{n0} + \frac{\hbar^2k^2}{2m_0} + \frac{\hbar^2}{m_0^2} \sum_{n' \neq n} \frac{|\langle u_{n0} | \mathbf{k} \cdot \mathbf{p} | u_{n'0} \rangle|^2}{\mathcal{E}_{n0} - \mathcal{E}_{n'0}}. \quad (1.116)$$

Note that the linear terms in k are not present since we are assuming that \mathcal{E}_{n0} represents a maximum or a minimum of the band structure. In Eqs. 1.115 and 1.116, the matrix elements $\langle u_{n0} | \mathbf{k} \cdot \mathbf{p} | u_{n'0} \rangle$ can be written as:

$$\langle u_{n0} | \mathbf{k} \cdot \mathbf{p} | u_{n'0} \rangle = \int u_{n0}^* \mathbf{k} \cdot \mathbf{p} u_{n'0} d\mathbf{r}. \quad (1.117)$$

Since \mathbf{k} is a vector of real numbers, these matrix elements can be rewritten as:

$$\langle u_{n0} | \mathbf{k} \cdot \mathbf{p} | u_{n'0} \rangle = \mathbf{k} \cdot \langle u_{n0} | \mathbf{p} | u_{n'0} \rangle. \quad (1.118)$$

For small values of k , it is very useful to write $\mathcal{E}_{n\mathbf{k}}$ as:

$$\mathcal{E}_{n\mathbf{k}} = \mathcal{E}_{n0} + \frac{\hbar^2k^2}{2m^*}, \quad (1.119)$$

where m^* is the effective mass. By comparing Eqs. 1.119 and 1.116, we obtain the following expression for the effective mass:

$$\frac{1}{m^*} = \frac{1}{m_0} + \frac{2}{m_0^2k^2} \sum_{n' \neq n} \frac{|\langle u_{n0} | \mathbf{k} \cdot \mathbf{p} | u_{n'0} \rangle|^2}{\mathcal{E}_{n0} - \mathcal{E}_{n'0}}. \quad (1.120)$$

This result is quite instructive since it states that the effective mass is not equal to the mass m_0 of the free electron as a result of the coupling between electronic states in different bands via the term $\mathbf{k} \cdot \mathbf{p}$. Moreover, the electron effective mass decreases upon decreasing the width of the gap $\mathcal{E}_{n0} - \mathcal{E}_{n'0}$ if the dominant term in Eq. 1.120 is given by the coupling between the conduction and valence bands.

As an example, from Eq. 1.116, it is possible to obtain an approximated expression of the dispersion curve for the conduction band assuming that \mathcal{E}_{n0} corresponds to the bottom of the conduction band, \mathcal{E}_{c0} . The sum over n' can include only the terms with energies close to the top of the valence band, where the energy difference at the denominator, $\mathcal{E}_{n0} - \mathcal{E}_{n'0}$

is smallest, since these terms give the most important contribution. Indeed, the relative importance of a band n' to the effective mass is controlled by the energy gap between the two bands. Therefore, we can reasonably assume:

$$\mathcal{E}_{n0} - \mathcal{E}_{n'0} = \mathcal{E}_{c0} - \mathcal{E}_{v0} = \mathcal{E}_g. \quad (1.121)$$

From Eq. 1.118, we have:

$$|\langle u_{n0} | \mathbf{k} \cdot \mathbf{p} | u_{n'0} \rangle|^2 = |\mathbf{k} \cdot \langle u_{c0} | \mathbf{p} | u_{v0} \rangle|^2 = k^2 |p_{cv}|^2, \quad (1.122)$$

where p_{cv} is the momentum matrix element between the two band edge Bloch functions:

$$p_{cv} = \langle u_{c0} | \mathbf{p} | u_{v0} \rangle = \int u_{c0}^*(\mathbf{r}) \mathbf{p} u_{v0}(\mathbf{r}) d\mathbf{r}. \quad (1.123)$$

Assuming the zero of the energy axis at the top of the dispersion curve, from Eq. 1.116 we can write:

$$\mathcal{E}_c(\mathbf{k}) = \mathcal{E}_{c0} + \frac{\hbar^2 k^2}{2m_0} + \frac{\hbar^2 k^2}{m_0^2} \frac{|p_{cv}|^2}{\mathcal{E}_g} = \mathcal{E}_g + \frac{\hbar^2 k^2}{2m_0} + \frac{\hbar^2 k^2}{m_0^2} \frac{|p_{cv}|^2}{\mathcal{E}_g}, \quad (1.124)$$

and from Eq. 1.120 we have:

$$\frac{1}{m^*} = \frac{1}{m_0} + \frac{2}{m_0^2} \frac{|p_{cv}|^2}{\mathcal{E}_g}. \quad (1.125)$$

A usually used parameter is the *Kane energy*:

$$\mathcal{E}_P = \frac{2}{m_0} |p_{cv}|^2, \quad (1.126)$$

so that the dispersion curve in Eq. 1.124 can be written as:

$$\mathcal{E}_c(\mathbf{k}) = \mathcal{E}_g + \frac{\hbar^2 k^2}{2m_0} \left(1 + \frac{\mathcal{E}_P}{\mathcal{E}_g} \right) \quad (1.127)$$

and the effective mass is:

$$\frac{1}{m^*} = \frac{1}{m_0} \left(1 + \frac{\mathcal{E}_P}{\mathcal{E}_g} \right). \quad (1.128)$$

The Kane energy is usually much larger than the energy gap and it is, to a good approximation, almost the same for most III–V semiconductors. Table 1.4 reports the Kane energy

Table 1.4 Kane energy values of a few semiconductors [1].

	\mathcal{E}_P (eV)
GaAs	28.8
AlAs	21.1
InAs	21.5
InP	20.7
GaN	25.0
AlN	27.1

values of a few semiconductors. For the conduction band of direct gap semiconductors, if the band gap decreases also the electron effective mass decreases. In other words, the bigger the energy gap, the smaller the effect on the effective mass. For example, in InSb the conduction band effective mass is very small, $m^* = m_0/77$ as a consequence of the very small energy gap $\mathcal{E}_g = 250$ meV.

1.8 Bandstructures of a Few Semiconductors

In this final section, we will briefly discuss relevant properties of the band structure of a few representative semiconductors. We will concentrate mainly on the characteristics of the band edges since most of the optical properties of the semiconductors are determined by regions of the band structure close to the top of the valence band and to the bottom of the conduction band. We will consider three semiconductors: Si, GaAs, and GaN.

1.8.1 Silicon

We have already mentioned that Si crystal has a diamond structure, with the first Brillouin zone in the form of a truncated octahedron, as shown in Fig. 1.11(b). Silicon is an indirect semiconductor. For this reason, it is not extensively used in optical devices. The top of the valence band is at the Γ -point, while the bottom of the conduction band is at the point $\frac{2\pi}{a}(0.85, 0, 0)$, close to the X -point (the direction [100] from the Γ -point to the X -point is called Δ -line). Since there are six equivalent Δ -lines, there are six equivalent minima in the conduction band at $k = \frac{2\pi}{a}(\pm 0.85, 0, 0)$, $\frac{2\pi}{a}(0, \pm 0.85, 0)$, and $\frac{2\pi}{a}(0, 0, \pm 0.85)$. The corresponding energy gap is 1.1 eV. The effective mass at these anisotropic minima is characterized by a longitudinal mass along the six equivalent [100] directions and two transverse masses in the plane orthogonal to the longitudinal direction. The longitudinal mass is $m_l = 0.98 m_0$, while the transverse mass is $m_t = 0.19 m_0$. The constant energy surfaces near the conduction band minima in Si can be written as:

$$\mathcal{E}(\mathbf{k}) = \frac{\hbar^2 k_x^2}{2m_l} + \frac{\hbar^2(k_y^2 + k_z^2)}{2m_t} \quad (1.129)$$

and are ellipsoids, as shown in Fig. 1.23. Equation 1.129 represents the parabolic band approximation. The direct energy gap is ~ 3.4 eV. There is also a second minimum in the conduction band at the point L , which is located about 1.1 eV above the band edge. The top of the valence band at the Γ -point presents the HH and LH degeneracy. The top of the split-off band is just 44 meV below the top of the valence band, as shown in Fig. 1.22(b). The LH mass is $m_{lh} = 0.16 m_0$, the HH mass is $m_{hh} = 0.46 m_0$, and the split-off hole mass is $m_{h,SO} = 0.29 m_0$.

1.8.2 Gallium Arsenide

Gallium arsenide is a III–V semiconductor. The electron configuration of isolated atoms is $[\text{Ar}]3d^{10}4s^24p^1$ for Ga and $[\text{Ar}]3d^{10}4s^24p^3$ for As. When forming a GaAs crystal, the

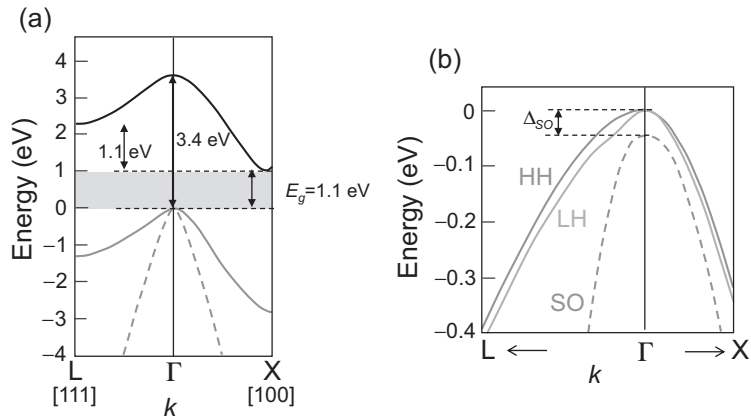


Figure 1.22 (a) Band structure of Si. (b) Zoom of a region of the valence band around the Γ -point, showing the heavy-hole (HH), the light-hole (LH), and split-off (SO) bands.

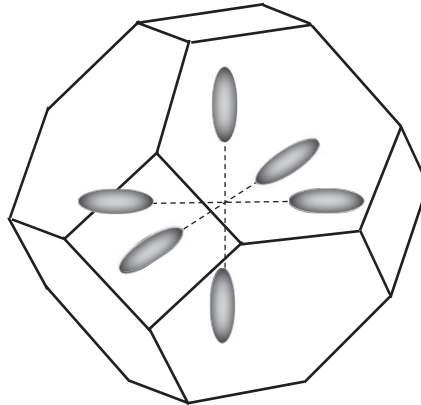


Figure 1.23 Constant energy surfaces near the conduction band minima in Si. There are six equivalent valleys in Si at the band edge.

outermost shell of each atom is hybridized in the form sp^3 so that each atom is surrounded by four neighbor atoms at the apex of a regular tetrahedron. GaAs is characterized by a zinc-blende crystal structure with a lattice constant $a = 5.65 \text{ \AA}$. GaAs is a direct band gap semiconductor, and it is largely used for optical devices (light-emitting diodes and lasers). The top of the valence band and the bottom of the conduction band are both at the Γ -point (see Fig. 1.20). The energy gap is 1.424 eV (at 300 K). The parabolic approximation for the conduction band is given by:

$$\mathcal{E}(k) = \frac{\hbar^2 k^2}{2m_c}, \quad (1.130)$$

where $m_c = 0.067 m_0$. In Eq. 1.130, we have assumed that at the band edge of the conduction band $\mathcal{E}(k) = 0$. When high fields are applied to the semiconductor, electrons can

be injected in states quite far from the minima. In this situation, the parabolic approximation does not hold any more and a better approximation for the conduction band is the following:

$$\mathcal{E}(1 + \alpha\mathcal{E}) = \frac{\hbar^2 k^2}{2m_c}, \quad (1.131)$$

with $\alpha = 0.67 \text{ eV}^{-1}$. The next highest minimum in the conduction band is close to the L -point. The separation between the Γ and L minima is 0.29 eV. The effective mass at the L minimum is much larger than the corresponding mass at the Γ -point: $m^* \approx 0.25 m_0$. The next higher energy minimum in the conduction band is at the X -point; the separation between the Γ and X minima is 0.48 eV. The corresponding electron effective mass is $m_X^* \approx 0.6 m_0$. When the semiconductor is subject to high electric fields, both the L and X valleys can be populated by electrons, in addition to the Γ valley. Therefore, these regions can be quite important to describe the electronic processes in GaAs. The valence band is characterized by the LH and HH bands and by the split-off band. The LH and HH masses are $m_{lh} = 0.082 m_0$ and $m_{hh} = 0.45 m_0$, respectively. The split-off energy is quite large: $\Delta = 0.34 \text{ eV}$, so that, in general, this band is always completely filled by electrons and does not play any relevant role in the electronic and optical properties of GaAs.

The temperature dependence of the energy gap can be well approximated by the following expression, the *Varshni equation*:

$$\mathcal{E}_g = \mathcal{E}_g(0) - \frac{\alpha T^2}{T + \beta}, \quad (1.132)$$

where T is the temperature (in K) and $\mathcal{E}_g(0)$ is the energy gap at $T = 0$. $\mathcal{E}_g(0)$, α and β are suitable fitting parameters, which are material-specific. In the case of GaAs $\mathcal{E}_g(0) = 1.519 \text{ eV}$, $\alpha = 5.405 \times 10^{-4} \text{ eV/K}$ and $\beta = 204 \text{ K}$. In the case of Si $\mathcal{E}_g(0) = 1.166 \text{ eV}$, $\alpha = 4.73 \times 10^{-4} \text{ eV/K}$ and $\beta = 636 \text{ K}$. This is a quite general behavior in semiconductors: The energy gap decreases upon increasing the temperature. It is possible to show that the temperature dependence of the energy gap is due to the electron–phonon interaction in the semiconductor, which depends on the amplitude of the phonons and on the corresponding coupling constants.

1.8.3 Gallium Nitride

Gallium nitride is another III–V semiconductor with a direct band gap, largely used in optoelectronic devices like light-emitting diodes and lasers. It has a large direct energy gap $\mathcal{E}_g = 3.45 \text{ eV}$, whose dependence on temperature can be taken into account by using the Varshni equation with $\mathcal{E}_g(0) = 3.51 \text{ eV}$, $\alpha = 9.09 \times 10^{-4} \text{ eV/K}$, and $\beta = 830 \text{ K}$ (in the range $293 \text{ K} < T < 1237 \text{ K}$). It usually presents the hexagonal wurtzite crystal structure. Also in this semiconductor, each atom presents sp^3 hybridization and forms tetrahedral bonds with its nearest neighbors, with a bonding angle of 109.47° and a bond length of 19.5 nm. The large energy gap is directly related to the large bonding strength in GaN. The first Brillouin zone of a hexagonal crystal is a hexagonal prism with height $2\pi/c$, as shown in Fig. 1.11(c). The spin–orbit splitting energy is $\Delta = 15.5 \text{ meV}$. The band structure

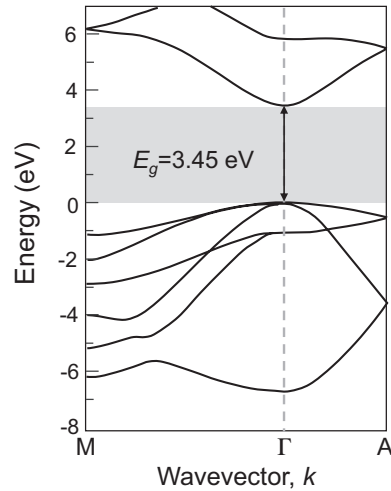


Figure 1.24 Calculated band structure of wurtzite GaN. Adapted with permission from [2].

of GaN near the band edges is shown in Fig. 1.24. The electron effective mass in the conduction band (Γ -minimum) is $m_c = 0.20 m_0$; in the valence band, the HH effective mass along the axis a is $m_{hh,a} = 1.65 m_0$, along the c -axis $m_{hh,c} = 1.1 m_0$, the LH masses are: $m_{lh,a} = 0.15 m_0$ and $m_{lh,c} = 1.1 m_0$.

1.9 Exercises

Exercise 1.1 The atomic packing factor is defined as the fraction of the volume of a crystal which is occupied by the constituent atoms, assumed as identical hard spheres centered on the atoms and with radius such that spheres on neighboring points just touch. Determine the atomic packing factor of the following crystal structures:

- simple cubic;
- body-centered cubic;
- face-centered cubic;
- hexagonal close-packed.

Exercise 1.2 The primitive translation vectors of the face-centered cubic lattice may be taken as:

$$\mathbf{a}_1 = \frac{a}{2}(\mathbf{u}_x + \mathbf{u}_y)$$

$$\mathbf{a}_2 = \frac{a}{2}(\mathbf{u}_y + \mathbf{u}_z)$$

$$\mathbf{a}_3 = \frac{a}{2}(\mathbf{u}_z + \mathbf{u}_x)$$

- a) determine the angles between these vectors;
- b) determine the volume of the primitive cell;
- c) determine the primitive translation vectors of the reciprocal lattice.

Exercise 1.3 Plot the Wigner–Seitz cell of a two-dimensional hexagonal lattice.

Exercise 1.4 Consider the momentum operator $\mathbf{p} = -i\hbar\nabla$ and the Bloch wavefunctions $\psi_{n\mathbf{k}}(\mathbf{r})$. Determine:

- a) $\mathbf{p}\psi_{n\mathbf{k}}$;
- b) $\mathbf{p}^2\psi_{n\mathbf{k}}$.

Exercise 1.5 By using the results of the previous exercise, write the Hamiltonian operator, $\mathbf{p}^2/2m + V(\mathbf{r})$, for the periodic function $u_{n\mathbf{k}}(\mathbf{r})$.

Exercise 1.6 Consider a monoatomic square lattice with only s -orbitals. Using the tight-binding method calculate and plot the dispersion curve ($\Gamma \rightarrow M \rightarrow X \rightarrow \Gamma$).

Exercise 1.7 A graphene lattice has two unit lattice vectors given by:

$$\begin{aligned}\mathbf{a}_1 &= 3/2L\mathbf{u}_x - \sqrt{3}/2L\mathbf{u}_y \\ \mathbf{a}_2 &= 3/2L\mathbf{u}_x + \sqrt{3}/2L\mathbf{u}_y\end{aligned}$$

- a) Determine the primitive vectors of the reciprocal lattice.
- b) Using the Wigner–Seitz algorithm, plot the first two-dimensional Brillouin zone and indicate the position vectors of all the corners. Indicate also the Γ point.
- c) Use the following dispersion relation for graphene:

$$\mathcal{E} = \pm t \sqrt{1 + 4 \cos\left(\frac{3L}{2}k_x\right) \cos\left(\frac{\sqrt{3}L}{2}k_y\right) + 4 \cos^2\left(\frac{\sqrt{3}L}{2}k_y\right)}$$

to plot the energy dispersion from Γ point to one of the corners ($t = 3 \text{ eV}$).

- d) What is the effective mass and velocity in the vicinity of the corner at $\mathcal{E} = 0$?
- e) Verify that it is a good estimate to write the energy dispersion at the corner (valley) as $\mathcal{E} = \hbar v k$. What is the valley degeneracy for graphene?

Exercise 1.8 Using a particular software (QUANTUM ESPRESSO) and the generalized gradient approximation (GGA), H.Q. Yang *et al.* have calculated the effective mass of the ternary alloy $\text{Ga}_x\text{In}_{1-x}\text{P}$ for Ga composition x varying from 0 to 1 [3]. The results are listed in Table 1.5:

- a) Plot the effective mass as a function of x .
- b) Write a polynomial fit for m^*/m_0 as a function of x . Note: for $0 \leq x \leq 0.625$, you can use a linear fit, while for $0.625 \leq x \leq 1$, you can use a parabolic fit. You will see that the curve $m^*(x)/m_0$ presents an inflection point at $x \approx 0.7$, where there is a change of the direct-to-indirect band gap for $\text{Ga}_x\text{In}_{1-x}\text{P}$.

Table 1.5 Effective mass of $\text{Ga}_x\text{In}_{1-x}\text{P}$, normalized to the free electron mass m_0 , versus Ga concentration x .

x	m^*/m_0
0	0.073060
0.125	0.089079
0.250	0.096235
0.375	0.105914
0.500	0.120593
0.625	0.133188
0.750	0.203615
0.875	0.412529
1	0.782270

Exercise 1.9 The velocity of an electron in a crystal can be written as $\mathbf{v} = (1/\hbar)\nabla_{\mathbf{k}}\mathcal{E}_n(\mathbf{k})$. Determine the velocity in the following two cases:

- a) parabolic band: $\mathcal{E}(\mathbf{k}) = \hbar^2 k^2 / 2m^*$;
 b) nonparabolic band: $\mathcal{E}(\mathbf{k})(1 + \alpha\mathcal{E}(\mathbf{k})) = \hbar^2 k^2 / 2m^*$.

Exercise 1.10 Assuming that $\mathcal{E} = \mathcal{E}_0 + 2\gamma \cos(ka)$, determine the electron position as a function of time (ignore scattering).

Exercise 1.11 Consider a simple cubic lattice (lattice spacing a), with one s -orbital per site. Assuming only nearest-neighbor interactions and neglecting overlap

a) show that the tight binding s -band is given by:

$$\mathcal{E}(\mathbf{k}) = \mathcal{E}_s - 2\gamma(\cos k_x a + \cos k_y a + \cos k_z a)$$

b) Plot the dispersion curve $\mathcal{E}(\mathbf{k})$ along directions $\Gamma - X - M - \Gamma - R$, where $X = \pi/a(1, 0, 0)$, $M = \pi/a(1, 1, 0)$, and $R = \pi/a(1, 1, 1)$.

Exercise 1.12 In a two-dimensional square lattice with lattice spacing a , the s -band can be written as:

$$\mathcal{E}(\mathbf{k}) = \mathcal{E}_s - 2\gamma(\cos k_x a + \cos k_y a).$$

- a) Determine the contours of constant energy near $k = 0$.
 b) Determine the contours of constant energy near the zone corners of the first Brillouin zone, showing that they are circles in the k -space. *Hint:* near the zone corners, k_x and k_y can be written as $k_x = (\pi/a) - \delta_x$ and $k_y = (\pi/a) - \delta_y$, with $\delta_{x,y}a \ll 1$.

Exercise 1.13 Write the tight-binding s -band, $\mathcal{E}(\mathbf{k})$, for a linear lattice (lattice spacing a), including a second-neighbor interaction, γ' .

Exercise 1.14 As first derived by Dresselhaus et al., the dispersion of the heavy- and light-hole bands at the top valence bands in diamond- and Zinc Blende-type semiconductors can be written as:

$$\mathcal{E}_{hh} = -Ak^2 - [B^2k^4 + C^2(k_x^2k_y^2 + k_y^2k_z^2 + k_z^2k_x^2)]^{1/2}$$

$$\mathcal{E}_{lh} = -Ak^2 + [B^2k^4 + C^2(k_x^2k_y^2 + k_y^2k_z^2 + k_z^2k_x^2)]^{1/2},$$

where the constants A , B , and C are related to the electron momentum matrix elements and to the energy gap. Determine the hole effective masses along the [100] and [111] directions.

Exercise 1.15 Plot the constant energy contour plot for the heavy-hole and light-hole dispersion reported in the previous exercise, in the plane (100) and (010).

Exercise 1.16 Calculate the density of wurtzite GaN. The lattice constants of GaN are $a = 3.186 \text{ \AA}$, $c = 5.186 \text{ \AA}$. The molar mass of GaN is 83.73 g/mol .

Exercise 1.17 Germanium has a diamond structure with a lattice constant $a = 5.64 \text{ \AA}$. Calculate the atomic density and the spacing between nearest-neighbor atoms.

Exercise 1.18 GaAs has a zinc-blende crystal structure. Assuming that the lattice spacing is $a = 5.65 \text{ \AA}$, calculate:

- the density of GaAs in g/cm^3 ;
- the density in atoms/cm^3 ;
- the valence electron number per unit volume;
- the closest spacing between adjacent As atoms.

Exercise 1.19 Consider a simple cubic semiconductor with lattice constant $a = 0.5 \text{ nm}$. The conduction and valence bands have the following dispersion curve along the k_x direction:

$$\mathcal{E}_c = A \left[1 - \frac{1}{2} \sin^2 \left(\frac{k_x a}{2} \right) \right]$$

$$\mathcal{E}_v = B [\cos(k_x a) - 1],$$

where $A = 1 \text{ eV}$ and $B = 0.5 \text{ eV}$.

- Plot the dispersion curves in the first Brillouin zone along the k_x direction and determine if the semiconductor is a direct or indirect band gap material.
- In the ideal case of absence of scattering, evaluate the maximum velocity along the X-direction of an electron in the valence band and specify the corresponding point in the first Brillouin zone.
- Evaluate the effective mass m_{xx} of the electron at the conduction band minimum and of the holes at the valence band maximum.

Exercise 1.20 Consider a tetragonal Bravais lattice with lattice parameters a , a and $c = 3a/4$, as shown in Fig. 1.25, where $a = 0.45 \text{ nm}$. Determine the reciprocal lattice vectors \mathbf{b}_1 , \mathbf{b}_2 , and \mathbf{b}_3 .

Exercise 1.21 Consider a two-dimensional hexagonal Bravais lattice, with lattice parameter $a = 0.5 \text{ nm}$, as shown in Fig. 1.26. The sites of the lattice are occupied by atoms with external s orbitals. The nearest-neighbor transfer integrals $\gamma = 0.15 \text{ eV}$ are assigned. All

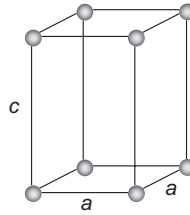


Figure 1.25 Tetragonal Bravais lattice.

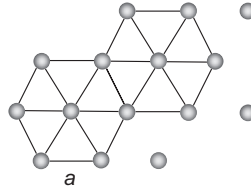


Figure 1.26 Two-dimensional hexagonal Bravais lattice, with lattice parameter $a = 0.5 \text{ nm}$.

other transfer integrals and all overlap integrals are negligible. The zero of the energy is set at the atomic level, $\mathcal{E}_s = 0$.

- Determine the dispersion $\mathcal{E}(\mathbf{k})$ of Bloch electrons within the tight-binding approximation, $\mathbf{k} = (k_x, k_y)$, being the wave vector.
- Determine the expression and numerical values of the elements of the inverse mass tensor m_{ij}^{-1} , with $i, j = x, y$, at the Γ point of the Brillouin zone.
- Determine the band width.